

PLANETARY CONSTRUCTION ZONES IN OCCULTATION: DISCOVERY OF AN EXTRASOLAR RING SYSTEM TRANSITING A YOUNG SUN-LIKE STAR AND FUTURE PROSPECTS FOR DETECTING ECLIPSES BY CIRCUMSECONDARY AND CIRCUMPLANETARY DISKS

ERIC E. MAMAJEK^{1,4}, ALICE C. QUILLEN¹, MARK J. PECAUT¹, FRED MOOLEKAMP¹, ERIN L. SCOTT¹,
MATTHEW A. KENWORTHY², ANDREW COLLIER CAMERON³, AND NEIL R. PARLEY³

¹ Department of Physics and Astronomy, University of Rochester, Rochester, NY 14627-0171, USA

² Leiden Observatory, Leiden University, P.O. Box 9513, 2300 RA Leiden, The Netherlands

³ School of Physics and Astronomy, University of St Andrews, North Haugh, St Andrews, Fife KY16 9SS, UK

Received 2011 August 19; accepted 2012 January 2; published 2012 February 10

ABSTRACT

The large relative sizes of circumstellar and circumplanetary disks imply that they might be seen in eclipse in stellar light curves. We estimate that a survey of $\sim 10^4$ young (~ 10 million year old) post-accretion pre-main-sequence stars monitored for ~ 10 years should yield at least a few deep eclipses from circumplanetary disks and disks surrounding low-mass companion stars. We present photometric and spectroscopic data for a pre-main-sequence K5 star (1SWASP J140747.93–394542.6 = ASAS J140748–3945.7), a newly discovered $\sim 0.9 M_{\odot}$ member of the ~ 16 Myr old Upper Centaurus–Lupus subgroup of Sco-Cen at a kinematic distance of 128 ± 13 pc. This star exhibited a remarkably long, deep, and complex eclipse event centered on 2007 April 29 (as discovered in Super Wide Angle Search for Planets (SuperWASP) photometry, and with portions of the dimming confirmed by All Sky Automated Survey (ASAS) data). At least five multi-day dimming events of >0.5 mag are identified, with a >3.3 mag deep eclipse bracketed by two pairs of ~ 1 mag eclipses symmetrically occurring ± 12 days and ± 26 days before and after. Hence, significant dimming of the star was taking place on and off over at least a ~ 54 day period in 2007, and a strong >1 mag dimming event occurring over a ~ 12 day span. We place a firm lower limit on the period of 850 days (i.e., the orbital radius of the eclipser must be >1.7 AU and orbital velocity must be <22 km s $^{-1}$). The shape of the light curve is similar to the lopsided eclipses of the Be star EE Cep. We suspect that this new star is being eclipsed by a low-mass object orbited by a dense inner disk, further girded by at least three dusty rings of optical depths near unity. Between these rings are at least two annuli of near-zero optical depth (i.e., gaps), possibly cleared out by planets or moons, depending on the nature of the secondary. For possible periods in the range 2.33–200 yr, the estimated total ring mass is $\sim 8\text{--}0.4 M_{\text{Moon}}$ (if the rings have optical opacity similar to Saturn’s rings), and the edge of the outermost detected ring has orbital radius $\sim 0.4\text{--}0.09$ AU. In the new era of time-domain astronomy opened by surveys like SuperWASP, ASAS, etc., and soon to be revolutionized by Large Synoptic Survey Telescope, discovering and characterizing eclipses by circumplanetary and circumsecondary disks will provide us with observational constraints on the conditions that spawn satellite systems around gas giant planets and planetary systems around stars.

Key words: binaries: eclipsing – planetary systems – planets and satellites: formation – planets and satellites: rings – stars: individual (1SWASP J140747.93–394542.6, ASAS J140748–3945.7) – stars: pre-main sequence

1. INTRODUCTION

The radii of circumstellar and circumplanetary disks can vastly exceed those of stars and planets. A companion star of a young stellar binary system can host a circumstellar disk, and likewise a giant planet in a young stellar system can host a circumplanetary disk. Because the disks are large, the probability that a randomly oriented system exhibits eclipses may not be negligible. These disks are particularly interesting as they could be seen in eclipse during the epoch of planet formation (in the case of a companion circumstellar disk; Galan et al. 2010) or during the epoch of satellite formation (in the case of a circumplanetary disk). In this paper, we consider the possibility of discovering eclipses by dust disks of low-mass companions in long-period orbits. With the advent of long-term and large-scale photometric surveys, strategies can be developed to discover young systems eclipsed by disks.

Some well-known long-period eclipsing systems have been interpreted in terms of occulting dark disks associated with an

orbiting companion, with the best examples being ϵ Aurigae (Guinan & DeWarf 2002; Kloppenborg et al. 2010; Chadima et al. 2011), EE Cep (Mikolajewski & Graczyk 1999; Graczyk et al. 2003; Mikolajewski et al. 2005; Galan et al. 2010), and the newly identified OGLE-LMC-ECL-17782 (Graczyk et al. 2011). EE Cep exhibits long (30–90 day) asymmetric eclipses with a period of 5.6 years and depth of $\sim 0.6\text{--}2.1$ mag. The primary object is a B5e giant star, and only primary eclipses are seen (Mikolajewski & Graczyk 1999). Structure seen in the wings of the eclipse has recently been interpreted in terms of rings and gaps in a forming planetary system around a lower mass secondary (Galan et al. 2010). ϵ Aurigae is the eclipsing system with the longest known period of 27.1 years. Only primary eclipses are seen, and they last almost two years. While the mass of the object hosting the dark occulting disk exceeds that of a visible F star, the masses of the two stars are not well constrained. However, emission lines and UV emission suggest that the hidden object is a B-type star (see discussion by Chadima et al. 2011). Infrared emission from the disk was detected with *IRAS* (Backman & Gillett 1985). OGLE-LMC-ECL-17782 (MACHO J053036.7–690625; Graczyk et al. 2011) is a 13 day eclipsing binary in the Large Magellanic Cloud (LMC)

⁴ Current address: Cerro Tololo Inter-American Observatory, Casilla 603, La Serena, Chile.

that demonstrates wide, flat-bottomed eclipses like ϵ Aur, but there are changes in the light curve from eclipse to eclipse, and transient features visible at other phases. Graczyk et al. (2011) suggest that the system is a detached binary⁵ where the secondary is “partially hidden within a semi-transparent, dark, elongated body or disk” and there are likely “transient structures in the system (disk debris?) responsible for additional minima at different orbital phases when one of the stars is hidden behind them.”

In this paper, we present the discovery of a solar-mass pre-main-sequence (pre-MS) non-accreting star exhibiting a long, unusual eclipse similar to those seen in EE Cep and ϵ Aurigae. The mass of the star and the lack of detected infrared emission suggest that the host object for the eclipsing disk is low mass, possibly a low-mass star, brown dwarf, or giant planet. Hence, we consider both *circumsecondary* and *circumplanetary disks* as possible occulting objects.

Why should one also consider *circumplanetary disks* associated with giant planets? First, natural satellites are a ubiquitous feature among the giant planets in our solar system, and most likely among extrasolar gas giants. The existence of such satellites and the H/He-rich atmospheres of gas giants hint that these planets likely formed with large gas and dust disks ($r_{\text{planet}} \ll r_{\text{disk}} < r_{\text{Hill}}$) that were originally accretion disks feeding from circumstellar material. These disks would then evolve passively after the circumstellar reservoir was depleted (Section 2), with matter accreting onto the planet, grain growth and proto-satellite accretion, and depletion through other mechanisms (e.g., Poynting–Robertson drag, radiation pressure, photoionization).

A simple thought experiment illustrates the potential observability of moon-forming circumplanetary disks around young gas giants (and indeed this was the back of the envelope calculation that spawned our interest in the interpretation of the eclipsing star discussed in Section 3). If one were to take the Galilean satellites of Jupiter, grind them up into dust grains, and spread the grains uniformly between Jupiter and Callisto’s orbit, one would have a dusty disk of optical depth $O(10^5)$. The size of such a proto-moon disk in this case would be a few solar radii—i.e., large enough and optically thick enough to potentially eclipse a star’s light. Of course, such a disk need not be face-on—more likely the disk would have a non-zero inclination with respect to the planet–star orbital plane, so the star need not be completely geometrically eclipsed by such a circumplanetary disk. The rings of Saturn have optical depth near ~ 1 even at a relatively old age (4.6 Gyr); however, the vast majority of mass orbiting Saturn is locked up in satellites ($M_{\text{rings}} \simeq 10^{-4} M_{\text{satellites}}$). Presumably a disk of much higher optical depth and significant radial substructure existed during the epoch of satellite formation. While there have been studies investigating the detectability of thin, discrete planetary rings similar to Saturn’s (e.g., Barnes & Fortney 2004; Ohta et al. 2009), there has been negligible investigation of the observability of the dense proto-satellite disks that likely existed during the first $\sim 10^7$ years. Relaxing the assumptions about the size, mass, composition, and structure of the disk in our back-of-the-envelope calculation has little impact on the feasibility of the

idea that *dusty disks of high optical depth may be a common feature of young gas giant planets, and such objects may be observable via deep eclipses of young stars.*

We first estimate the timescale of an eclipse by a circumsecondary or circumplanetary disk in Section 2. This is done first so that the photometric light curve of our object can be interpreted in terms of eclipse models. We then present and discuss the properties of our candidate long-period eclipsing system in Section 3. In Section 4, we discuss the probability of detecting eclipses using time-series photometry of large samples of young stars. A discussion and summary follow in Section 5.

2. CIRCUMSECONDARY AND CIRCUMPLANETARY DISK ECLIPSES

The multiplicity of class I young stellar objects (YSOs) in embedded clusters and pre-MS stars in young associations is high and ranges from 20% to 60% for the $\sim 10^{1.5}$ – $10^{2.5}$ AU separation range and mass ratios of ~ 0.1 – 1 (see the comprehensive review by Duchêne et al. 2007 and also Kraus et al. 2011). Among the binaries found in young clusters, stars in different stages of disk evolution are not rare (Hartigan & Kenyon 2003; McCabe et al. 2006; Monin et al. 2007; Prato & Weinberger 2010). These binaries, known as “mixed pairs,” have one star hosting a disk or actively accreting and the other lacking a disk or signatures of accretion. While the two most well-known long-period eclipsing disk systems (EE Cep and ϵ Aurigae) involve massive stars, the large fraction of binary systems in young associations and clusters suggests that long-period eclipsing circumsecondary disk systems may be discovered in lower mass systems.

Recent explorations of circumplanetary disks separate the disk evolution into two phases (Alibert et al. 2005; Ward & Canup 2010). In the first phase the circumplanetary disk is fed by material from the circumstellar disk and the circumplanetary disk acts like an accretion disk. In the second phase the circumstellar disk has dissipated, and the viscosity of the circumplanetary disk both drives accretion onto the planet and causes the disk to spread outward. The lack of differentiation of Callisto (Anderson et al. 1996) suggests that the accretion or formation timescale for all the Galilean satellites was prolonged (Canup & Ward 2002) and would have happened during the second phase of evolution after the circumstellar disk dissipated (Canup & Ward 2002; Alibert et al. 2005; Ward & Canup 2010; Mosqueira et al. 2010). Also, modeling of Iapetus, the outermost regular satellite of Saturn, suggests that it formed 3–5 Myr after the formation of Ca–Al inclusions (Castillo-Rogez et al. 2009). Since Iapetus survived Type I migration, it must have formed near the end of substantial accretion onto Saturn from the circumsolar nebula. Mosqueira et al. (2010) suggest that Iapetus’ large separation from Saturn’s principal satellite Titan is suggestive that the remnant circum-Saturnian nebula may have had two components: a dense inner disk that spawned most of Saturn’s regular satellites, out to the centrifugal radius near Titan, and a disk of much lower density beyond the centrifugal radius—perhaps to Phoebe’s orbit. Because of the extended estimated circumplanetary disk lifetime, we can consider the possibility that circumplanetary disks can be seen in eclipse against a young central star after the dissipation of the circumstellar disk.

We consider two bodies with masses m_1, m_2 in a circular orbit with semi-major axis a_B and mass ratio $\mu \equiv m_2/m_1 + m_2$. In the case of a stellar binary, the more massive star is m_1 and the secondary is m_2 . In the case of a system with a single planet, m_2

⁵ The author dereddened the *UBV* photometry for OGLE-LMC-ECL-17782 from Massey (2002, cataloged as M2002 148104) using the Q-method and finds that the primary is most likely a slightly evolved $\sim B2$ star with $(B - V)_0 \simeq -0.23$ and $M_V \simeq -3.7$. However, this calculation does not take into account the difference in metallicities between LMC and local Galactic massive stars.

Table 1

Hill Radii and Orbital Radii of Outermost Regular Satellites for Large Planets

(1) Planet	(2) r_H (AU)	(3) v_{orb} (km s ⁻¹)	(4) Outermost Reg. Sat.	(5) r_{sat}/r_H	(6) t_{transit} (days)
Jupiter	0.36	13.1	Callisto	0.035	3.3
Saturn	0.44	9.7	Iapetus	0.054	8.5
Uranus	0.47	6.8	Oberon	0.008	2.0
Neptune	0.78	5.4

Notes. Column 2 is the Hill radius r_H in AU, column 3 is the planet’s mean orbital velocity in km s⁻¹, column 4 is the name of the outermost large regular satellite for each planet, column 5 is the ratio of that moon’s orbital radius to the Hill radius, and column 6 is the timescale t_{transit} for a circumplanetary disk with outer radius equal to the orbital radius of the outermost large regular satellite to transit in front of the Sun, given the planet’s orbital velocity. Neptune does not have a system of large regular satellites. Its principal moon, Triton, is in a retrograde orbit and was likely captured as a component of a binary dwarf planet (Agnor & Hamilton 2006).

is the mass of the planet and m_1 is the mass of the central star. The masses and semi-major axis set the Hill or tidal radius of the secondary $r_H \equiv a_B(\mu/3)^{1/3}$.

A disk surrounding m_2 is described with two parameters, the radius at which its optical depth is of order unity, r_d , and the obliquity or axial tilt of the disk system, ϵ , with respect to the axis defining the orbital plane. The angle ϵ is zero for a disk that lies in the orbital plane. It is convenient to define a size ratio $\xi \equiv r_d/r_H$ that represents the size of the disk in Hill or tidal radii.

Studies of giant planets have made estimates for the size ratio ξ . Based on a centripetal radius argument, Quillen & Trilling (1998) estimated that an accreting circumplanetary disk would have $\xi = 1/3$. Hydrodynamic simulations of planets embedded in circumstellar disks also can find $\xi \sim 0.3$ (Ayliffe & Bate 2009). A tidal truncation argument suggests $\xi \sim 0.4$ (Martin & Lubow 2011). Theoretical models for Jupiter’s circumplanetary disk accounting for Galilean satellite formation after the dissipation of the circumstellar disk estimate smaller radii of $\xi \sim 0.1$ – 0.2 (Canup & Ward 2002; Magni & Coradini 2004; Ward & Canup 2010). For reference, the outermost of the Galilean satellites, Callisto, currently has a semi-major axis that is only a small fraction of Jupiter’s Hill radius $a \approx 0.0355r_H$. Jupiter’s Hill radius is about $743R_{\text{Jup}}$, where R_{Jup} is the radius of Jupiter. Estimates of the Hill radii r_H and the ratio of the orbital radii to Hill radii (r_{sat}/r_H) for the outermost large, regular satellites for the giant planets in our solar system are summarized in Table 1. Column 6 of Table 1 estimates the timescale for a circumplanetary disk with outer radius equal to the orbital radius of the outermost regular satellite to transit in front of the Sun, given the planet’s mean orbital velocity.

The results suggest that substantial circumplanetary disks of sufficient surface density for satellites to accrete must have existed around the giant planets in our solar system for some period during the post-T Tauri phase for our Sun. These circumplanetary disks likely had outer radii of $\xi > 0.01$ – 0.05 and could have been detectable by eclipses with ~ 1 – 10 day timescales to observers along opportune lines of sight.

A disk in a binary system might extend all the way to its Roche radius (Lin & Papaloizou 1993; Artymowicz & Lubow 1994; Andrews et al. 2010) with $\xi \sim 1$. For example, the disk of HD 141569A (Clampin et al. 2003) may extend to its Roche radius when the secondary is at pericenter and approaches

HD 141569A (Augereau & Papaloizou 2004; Quillen et al. 2005). The truncated disks of HD 98800 and Hen 3-600 are consistent with tidal truncation (Andrews et al. 2010).

A circular orbit for m_2 would have a circumference of $\sim 2\pi a_B$. The disk extends a distance $\pm r_d \sin \epsilon$ above and below the orbital plane. Thus, the area of a cylinder that could be intersected by an eclipsing line of sight is $A \sim 4\pi a_B r_d \sin \epsilon$. Here we have neglected the thickness of the disk at low obliquity. If the disk is seen edge-on, then $A \sim 4\pi a_p h_d$, where h_d is the scale height of the disk near its opacity edge. We can define a factor

$$y(\epsilon) = \max\left(\frac{h_d}{r_d}, \sin \epsilon\right). \quad (1)$$

To estimate the probability that a system containing a disk is oriented so that it would exhibit eclipses, we divide this area by $4\pi a_p^2$:

$$p_{\text{orient}} \sim \frac{r_d y(\epsilon)}{a_B} \sim \xi \mu^{1/3} 3^{-1/3} y(\epsilon). \quad (2)$$

This probability is independent of the binary or planet’s semi-major axis.

Studies of primordial circumplanetary disks have calculated their thermal structure (Canup & Ward 2002; Alibert et al. 2005). The circumplanetary disk aspect ratio h/r is predicted to be in the range 0.1–0.3, where h is the vertical scale height a radial distance r from the planet’s center (e.g., see Figure 9 of Alibert et al. 2005). Hydrostatic equilibrium relates the temperature T of a gaseous disk to its vertical scale height and the speed Ω of objects in orbit $h \sim c_s/\Omega$, where sound speed $c_s = (kT)^{1/2}(\mu m_H)^{-1/2}$, k is Boltzmann’s constant, μ is the mean molecular weight, and m_H is the mass of hydrogen). Owing to the low circular velocities for objects in orbit about a planet, a gaseous circumplanetary disk would not have a small aspect ratio until its gas has dissipated.

The temperature and scale height of a circumstellar disk are set from the dominant source of heat, which is from absorption of stellar radiation unless the accretion rate is high. A good rough guideline covering a wide range of conditions is aspect ratio $h/r \sim 0.05$ – 0.1 (e.g., see Figure 1 by Edgar et al. 2007). The factor $y(\epsilon)$ also depends on the orientation of the disk. Strongly misaligned disks should be brought into rough alignment by shocks associated with tidal torques in only about 20 binary orbital periods (Bate et al. 2000). For modest misalignment angles, misalignment can persist over considerably longer periods. Disks have been imaged in wide binary T Tauri stars that are misaligned with the binary orbital plane (e.g., HK Tau; Stapelfeldt et al. 1998). If the system is not a binary but a triplet or a quadruple system, then misalignment may be more common (as discussed by Prato & Weinberger 2010). Prato & Weinberger (2010) emphasize (see their Section 4) that “even binaries with separations of a few tens of AU—or less—cannot be assumed to harbor aligned disks coplanar with binary orbits.” Hence, the obliquity distribution for circumsecondary disks may be wide.

Evaluating Equation (2) with illustrative parameters, we estimate that the fraction of randomly oriented systems (at a given mass ratio) hosting a disk that are oriented so they could exhibit an eclipse is

$$f_{\text{orient}} \sim 0.004 \left(\frac{\xi}{0.2}\right) \left(\frac{m_2}{M_J}\right)^{1/3} \left(\frac{m_1 + m_2}{M_\odot}\right)^{-1/3} \left(\frac{\bar{y}}{0.3}\right). \quad (3)$$

Here we have taken \bar{y} to be the mean of the distribution of $y(\epsilon)$ that depends on the obliquity and disk height distribution

and M_J is the mass of Jupiter. Because of the large size of a circumplanetary or circumsecondary disk, the fraction f_{orient} of objects capable of giving eclipses, and that such eclipses will be seen, is not low.

The timescale for the eclipse to occur will depend on the angular rotation rate of the orbit,

$$t_{\text{eclipse}} \sim \sqrt{\frac{a_B^3}{G(m_1 + m_2)}} \frac{2r_d}{a_B} \sim P \xi \mu^{1/3} \pi^{-1} 3^{-1/3} \\ \sim 1.5 \text{ days} \left(\frac{\xi}{0.2}\right) \left(\frac{m_2}{M_J}\right)^{1/3} \left(\frac{m_1 + m_2}{M_\odot}\right)^{-1/3} \left(\frac{a_B}{1 \text{ AU}}\right)^{3/2}, \quad (4)$$

where we have assumed that the radius of the occulted object $R_1 \ll r_d$ and P is the orbital period of the planet or binary.

The fraction of the orbit spent in eclipse is

$$f_{\text{eclipse}} = \frac{t_{\text{eclipse}}}{P} \sim \xi \mu^{1/3} \pi^{-1} 3^{-1/3} \quad (5)$$

and is independent of the semi-major axis.

Once a disk eclipse candidate is identified, one could search for reflected starlight from the disk. The area intersecting light from the star is $A \sim 4\pi r_d^2 \sin y(\epsilon)c$, where the order unity factor c depends on the orientation of the disk. The fraction of reflected starlight would be

$$f_r \sim \left(\frac{r_d}{a_p}\right)^2 y(\epsilon)c' \sim \xi^2 \mu^{2/3} y(\epsilon)c', \quad (6)$$

where the order unity factor c' depends on c , the disk's albedo, and the dependence on scattering angle. The difference in magnitude between the reflected light of the disk and the star is

$$\delta m \sim 9.8 - 2.5 \log_{10} \left[\left(\frac{\xi}{0.2}\right)^2 \left(\frac{\mu}{10^{-3}}\right)^{2/3} \left(\frac{y(\epsilon)c'}{0.3}\right) \right]. \quad (7)$$

This level of magnitude difference is not extremely high, suggesting that it may be feasible to detect reflected light from circumplanetary disks with an adaptive optics system.

2.1. Disk Lifetimes

For young binary systems in nearby star-forming regions (with typical ages of <3 Myr) the estimated fraction of mixed systems with the primary a weak-lined T Tauri star and the secondary a classical T Tauri star is not low and could be as large as $\sim 1/3$ (Monin et al. 2007). The mixed systems imply that the circumstellar disks around the primary and secondary can have lifetimes that differ by a factor of about two (Monin et al. 2007). A tidally truncated disk around a low-mass secondary is expected to have a shorter accretion lifetime than the primary's disk (Armitage et al. 1999); however, there are other environmental factors such as dispersal of the host molecular cloud, birth cluster density, and disk evaporation that can influence multiplicity and disperse disks (Monin et al. 2007; Prato & Weinberger 2010).

We can estimate the lifetime of a circumplanetary disk by scaling from models for the proto-Jovian disk. The orbital period of a particle in orbit about a planet with radius near the Hill radius is approximately that of the planet in orbit about the star. The lifetime of a circumplanetary disk likely depends on the orbital

period at its outer edge and so depends on $\xi^{3/2}$ times the planet's orbital period. If ξ is similar for different circumplanetary disks, the lifetime of the secondary phase of these disks (after circumstellar disk dissipation) should be proportional to the planet's semi-major axis to the $3/2$ power. We can use this scaling relation to estimate the lifetime of circumplanetary disks at larger distances from the star than Jupiter. The lifetime of the second phase of Jupiter's circumstellar disk is estimated to be of order a million years (Canup & Ward 2002; Alibert et al. 2005; Ward & Canup 2010). We estimate that the lifetime of a circumplanetary disk at 25 AU could be about 10 times longer (or of order 10^7 years) and at 100 AU (such as Fomalhaut b) 100 times longer (or of order 10^8 years).

The planet Fomalhaut b has been detected in two visible bands only (Kalas et al. 2008). While the detected object is in orbit about Fomalhaut, its color is consistent with that of reflected light from the star. These observations led Kalas et al. to suggest that the planet hosts a circumplanetary ring akin to Saturn's (see Arnold & Schneider 2004), which would extend to at least 20 Jupiter radii for an assumed albedo of 0.4 to recover the observed fluxes. Another possibility is that this is reflected light from a gaseous circumplanetary disk. Owing to the large semi-major axis of the planet (and so large Hill radius), the lifetime of this disk would exceed that estimated for Jupiter's circumplanetary disk, making this possibility more tractable. The light from Fomalhaut b is unresolved so the emitting object must be confined to a region smaller than the *Hubble Space Telescope* Advanced Camera point-spread function (PSF) FWHM of 0.5 AU (Kennedy & Wyatt 2011). The ratio of 0.5 AU to the planet's semi-major axis of 119 AU gives a constraint $\xi^3 \mu = 2.2 \times 10^{-7}$. For $\xi = 0.2$ this gives a planet mass ratio of 2×10^{-5} and for $\xi = 0.1$ of 2×10^{-4} , hence ranging from Saturn to Neptune mass and lower than estimated by Chiang et al. (2009) but consistent with that predicted by Quillen (2006).

3. A CANDIDATE ECLIPSING DISK

3.1. The Star

We are currently conducting a large-scale spectroscopic survey for new low-mass members of the Sco-Cen OB association (M. J. Pecaut & E. E. Mamajek 2012, in preparation) using the RC spectrograph on the SMARTS⁶ 1.5 m telescope at Cerro Tololo. Sco-Cen is the nearest OB association to the Sun (mean subgroup distances of $d \simeq 118$ –145 pc; de Zeeuw et al. 1999) and consists of three subgroups with ages of ~ 11 –17 Myr (Pecaut et al. 2011; Preibisch & Mamajek 2008). The survey sample consisted of ~ 350 stars with optical/near-IR colors consistent with having K/M spectral types, PPMX proper motions (Roeser et al. 2008) consistent with membership to the three Sco-Cen subgroups, and X-ray emission detected in the *ROSAT* All-Sky Survey (Voges et al. 1999, 2000). The photometric and astrometric survey PPMX catalog (Roeser et al. 2008) is complete down to $V \simeq 12.8$ mag with typical astrometric accuracy of 2 mas yr^{-1} . The survey sample was cross-referenced with the stars with light curves in the first public data release (DR1) of the Super Wide Angle Search for Planets (SuperWASP) public archive⁷ (Butters et al. 2010). SuperWASP is a photometric sky survey for detecting transiting extrasolar planets with instruments in La Palma and in South Africa, which have continuously monitored

⁶ <http://www.astro.yale.edu/smarts/>

⁷ <http://www.wasp.le.ac.uk/public/>

Table 2
Properties of Star

(1) Property	(2) Value	(3) Ref
α (J2000)	14:07:47.93	1
δ (J2000)	-39:45:42.7	1
μ_α	-25.4 ± 1.4 mas yr $^{-1}$	1
μ_δ	-20.1 ± 3.5 mas yr $^{-1}$	1
Spec. type	K5 IV(e) Li	2
$E(B - V)$	0.09 mag	2
A_V	0.32 mag	2
Dist	128 ± 13 pc	2
EW(H α)	0.2 Å (emis.)	2
EW(Li I λ 6707)	0.4 Å (abs.)	2
T_{eff}	4500^{+100}_{-200} K	2
$\log(L/L_\odot)$	-0.47 ± 0.11 dex	2
R	$0.96 \pm 0.15 R_\odot$	2
X-ray flux	3.59×10^{-2} counts s $^{-1}$	3
HR1	-0.04 ± 0.42	3
$\log(L_X/L_{\text{bol}})$	-3.4	2, 3
L_X	$10^{29.8}$ erg s $^{-1}$	2, 3
P_{rot}	3.20 days	2
Age	~ 16 Myr	2
Mass	$0.9 M_\odot$	2

References. (1) Zacharias et al. 2010; (2) this paper; (3) Voges et al. 2000.

the sky since 2004, and the DR1 contains nearly 18 million light curves (Pollacco et al. 2006). Of our ~ 350 Sco-Cen survey stars, at least 200 appear to be new bona fide pre-MS stars, and SuperWASP light curves were available for 138 of them.

Among the SuperWASP DR1 data for the new Sco-Cen members, we⁸ identified a star with a remarkable light curve (PPMX J140747.9-394542 = GSC 7807-0004 = 1SWASP J140747.93-394542.6 = 3UC 101-141675 = 2MASS J14074792-3945427, hereafter “J1407”). The light curve is dominated by a quasi-sinusoidal component with amplitude ~ 0.1 mag in the WASP-V photometric band, with periodicity of 3.21 days (consistent with rotational modulation of starspots, typical for young active stars), and a deep eclipse with maximum depth ~ 3 mag between HJD 2454213 (2007 April 23) and HJD 2454227 (2007 May 7), with a complex pattern of roughly symmetric dimming and brightening within ± 26 days of 2007 April 29 HJD 2454220. The properties of this star are listed in Table 2, and the relevant optical/IR photometry is listed in Table 3. We discuss the eclipse further in Section 3.2.

The spectral energy distribution for the star (plotted in Figure 1) is consistent with a lightly reddened K5 star ($E(B - V) = 0.09$, $A_V \simeq 0.32$ mag), with no evidence for infrared excess (via Two Micron All Sky Survey (2MASS) and *Wide-field Infrared Survey Explorer* (WISE) preliminary release photometry; Skrutskie et al. 2006; Wright et al. 2010). Using a low-resolution red spectrum taken in 2009 July with the SMARTS 1.5 m telescope RC spectrograph, shown in Figure 2, we classify the star as *K5IV(e) Li*, i.e., a Li-rich K star with negligible H α emission (0.2 Å equivalent width; i.e., “filled-in”) and Na doublet feature that is weaker than that for dwarfs, but not consistent with a giant either (so we adopt intermediate-luminosity class IV; Keenan & McNeil 1989).

The star is located in the vicinity of the Upper Centaurus-Lupus (UCL) subgroup of the Sco OB2 association

⁸ The deep SuperWASP eclipse for this star was first noticed on 2010 December 3 by Pécaut & Mamajek.

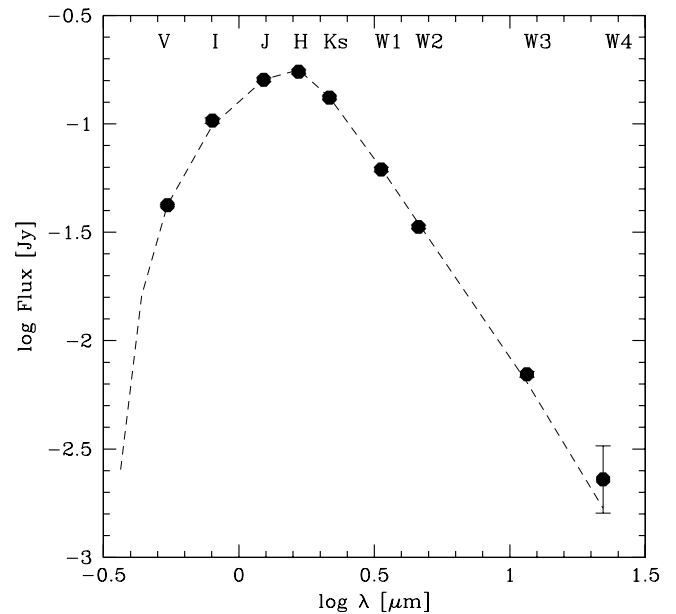


Figure 1. Observed photometry for J1407 taken from Table 3 (filled circles) compared to the spectral energy distribution for a lightly reddened K5 dwarf with $E(B - V) = 0.09$ (dashed line). We have assumed that the K_s minus WISE band (W1, W2, W3, W4) colors are zero.

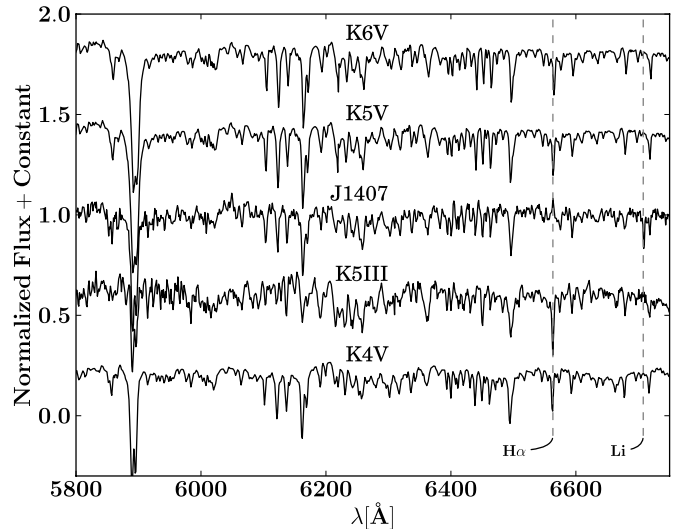


Figure 2. Comparison of CTIO 1.5 m red optical spectrum of J1407 with CTIO spectra of four spectral standard stars from Keenan & McNeil (1989): TW PsA (K4V), N Vel (K5III), HD 36003 (K5V), and GJ 529 (K6Va).

(de Zeeuw et al. 1999), and its proper motion is statistically consistent with moving toward the UCL convergent point (a negligible peculiar velocity of 0.9 ± 1.8 km s $^{-1}$), with a kinematic distance of 128 ± 13 pc (similar to other UCL members).⁹ Using this distance, we place the star on the H-R diagram (see Figure 3; $\log T$, $\log L/L_\odot = 3.66$, -0.47). Factoring in the ± 0.11 dex uncertainty in $\log(L/L_\odot)$, dominated by the distance uncertainty, the isochronal ages and their uncertainties are listed in Table 4. Factoring in previous age estimates for the UCL subgroup (see summary in Mamajek et al. 2002) and new age estimates using the F-star MS turn-on (Pécaut et al. 2011),

⁹ The distance and peculiar velocity were calculated following Mamajek (2005), using the UCAC3 proper motion for J1407 and the updated estimate of the mean space motion for UCL from Chen et al. (2011): (U , V , W) = (-5.1 ± 0.6 , -19.7 ± 0.4 , -4.6 ± 0.3) km s $^{-1}$.

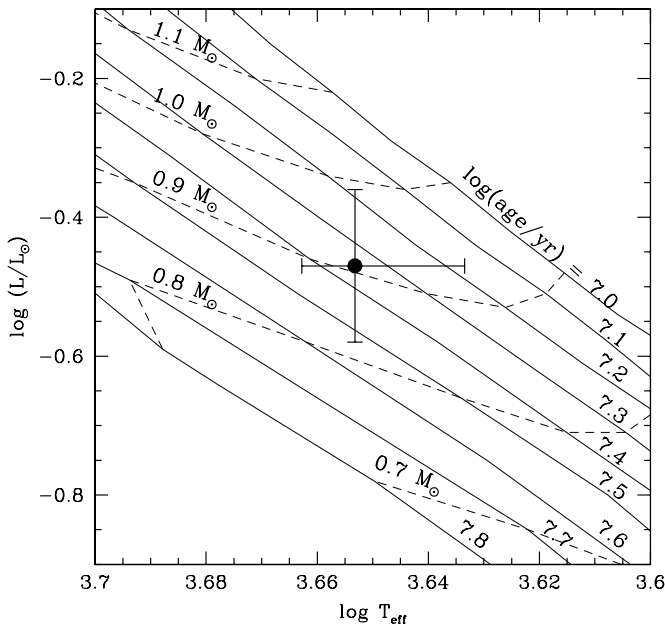


Figure 3. H-R diagram position for star J1407 with isochrones in $\log(\text{age}/\text{yr})$ from Baraffe et al. (1998) overlain.

Table 3
Photometry of Star

(1)	(2)	(3)	(4)
Band	λ_o	Mag	Ref
V	0.55 μm	12.31 \pm 0.03	1
I	0.79 μm	10.92 \pm 0.03	2
J	1.24 μm	9.997 \pm 0.022	3
H	1.66 μm	9.425 \pm 0.023	3
K _s	2.16 μm	9.257 \pm 0.020	3
W1	3.4 μm	9.252 \pm 0.025	4
W2	4.6 μm	9.276 \pm 0.021	4
W3	12 μm	9.141 \pm 0.033	4
W4	22 μm	8.907 \pm 0.388	4

Notes. (1) V band is the median of SuperWASP and ASAS measurements out of eclipse, given equal weight to both data sets, and the ± 0.03 mag is a systematic uncertainty. The SuperWASP photometry was converted to Johnson V using factors by Bessell (2000) and assuming $V_{\text{SuperWASP}} = V_{\text{Tycho}}$ (Pollacco et al. 2006), (2) DENIS (The DENIS Consortium 2005), (3) 2MASS (Cutri et al. 2003), and (4) WISE first data release (Wright et al. 2010).

Table 4
Isochronal Age and Mass Estimates for J1407

(1)	(2)	(3)
Age (Myr)	Mass (M_{\odot})	Models (...)
23 ⁺¹⁴ ₋₉	0.90 \pm 0.08	1
27 ⁺¹⁵ ₋₁₀	0.89 \pm 0.07	2
14 ⁺¹¹ ₋₆	0.86 \pm 0.06	3

Notes. References for the models are as follows: (1) Baraffe et al. 1998; (2) Siess et al. 2000; (3) D’Antona & Mazzitelli 1997.

we estimate the mean age of UCL to be 16 Myr with a ± 2 Myr (68% CL) systematic uncertainty. The isochronal age for J1407 is consistent with this value; hence, we adopt the mean UCL age

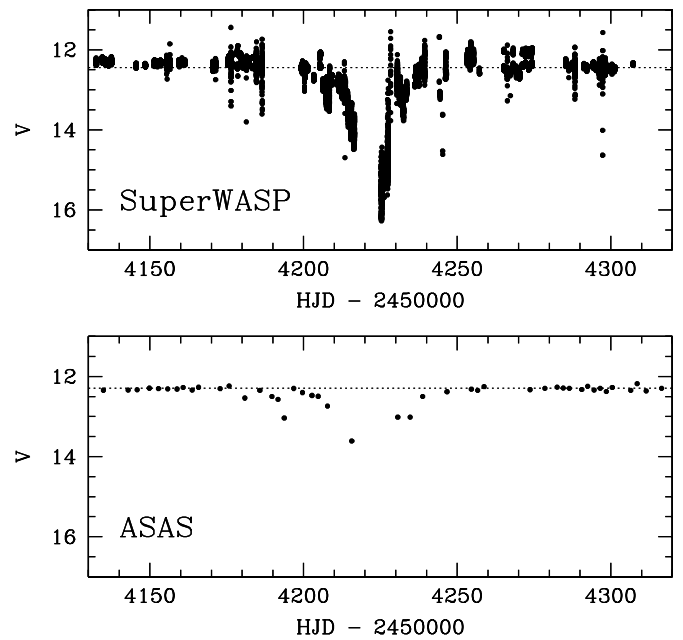


Figure 4. Individual measurements of SuperWASP (top) and ASAS (bottom) V magnitudes for J1407 during early 2007. The abscissa is Heliocentric Julian Date minus 2450000. 2007 January 1 midnight corresponds to HJD 2454101.5. The eclipse was seen in both photometric data sets. The eclipse was deep for about 14 days but is bookended by a gradual dimming covering a period of about ± 54 days. Long-term median magnitudes outside of eclipse are plotted with dotted lines ($V = 12.29$ for ASAS, $V = 12.45$ for SuperWASP). The systematic difference is mostly due to SuperWASP-V being calibrated to the Tycho V_T band (Pollacco et al. 2006), whereas the ASAS is converted to the Johnson V system via *Hipparcos* (Pojmanski 2002).

as the age for J1407. Three sets of evolutionary tracks predict similar masses for J1407: $\sim 0.9 M_{\odot}$ (listed in Table 4).

The kinematics of the star, rotation period (as discussed below), X-ray emission, and its preliminary H-R diagram position are mutually self-consistent with the interpretation that this star is a nearby (distance ~ 130 pc), $\sim 10^7$ yr old, solar-mass pre-MS star.

3.2. Light Curves

The V-band light curve for J1407 during the year of 2007 from the All Sky Automated Survey (ASAS; Pojmanski 2002) and SuperWASP surveys is shown in Figure 4. The SuperWASP survey is an ultra-wide field (over 300 deg²) photometric survey designed to monitor stars between $V \sim 7$ and 15 mag to search for transiting extrasolar planets (Pollacco et al. 2006). The public data archive of SuperWASP photometry is described in Butters et al. (2010). The SuperWASP DR1 photometry for J1407 contains photometry for approximately 29,000 epochs during 206 dates between HJD 2453860 (2006.34) and HJD 2455399 (2010.56), with median photometric precision of 0.023 mag. The light curve for J1407 from the SuperWASP data¹⁰ is dominated by (1) a sinusoidal component with amplitude ~ 0.1 mag in the WASP-V photometric band, with periodicity of 3.211 days (consistent with rotational modulation of starspots, typical for young active stars, e.g., Mamajek & Hillenbrand 2008), and (2) a 14 day deep eclipse of depth $\gtrsim 3$ mag between dates HJD 2454213 (2007 April 23) and HJD 2454227 (2007 May 7), bookended by gradual dimmings and brightenings to the median brightness (Figure 4). The same light curve is also shown

¹⁰ Can be retrieved from <http://www.wasp.le.ac.uk/public/lc/index.php> with the identifier 1SWASP J140747.93–394542.6.

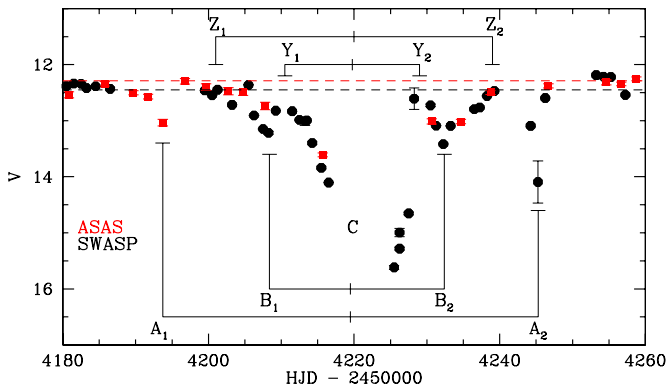


Figure 5. SuperWASP and ASAS photometry for the 2007 April–May eclipse event(s). ASAS photometry is a single measurement each night, whereas the SuperWASP magnitudes are nightly median values (the standard error of the median is plotted). The four (two pairs) peripheral dips are labeled and matched to their partner. The midway dates for both the “A” and “B” dips coincide within a day of HJD 2454220 (2007 April 29). Dips A_1 and A_2 are ~ 51.5 days apart, and dips B_1 and B_2 are ~ 24 days apart. Periods of low extinction are labeled Z_1 and Z_2 and Y_1 and Y_2 .

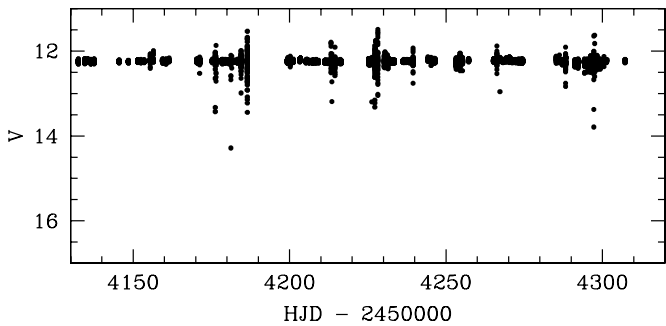


Figure 6. SuperWASP light curve for the comparison star 1SWASP J1407252.03–394415.1 (GSC 07807-00572), a star of similar brightness ($V = 12.24$) to J1407 and situated $99'6$ away from it. The time span covers the same range as the light curve for J1407 in Figure 5. A total of 7829 photometric data points with median photometric error ± 0.018 mag are shown, and 68% (95%) are within ± 0.021 (0.077) mag of $V = 12.245$. Despite the appearance of some discrepant photometric points (with correspondingly large photometric errors), there is no evidence for any complex behavior similar to that seen for J1407.

in Figure 5 using median nightly SuperWASP values. In Figure 6 we plot the SuperWASP light curve for a comparison field star situated $\sim 100''$ away from J1407 and of similar brightness (plotted over the same time period as J1407’s eclipse and the same magnitude scale as in Figure 5). There is no evidence for similar complex behavior during the epoch of J1407’s eclipse in the light curve for the comparison star. We discuss various scenarios for explaining the dimming of J1407 in Section 3.6.

The ASAS-3 archive also contained an extremely long time-baseline light curve for J1407 (ASAS J140748–3945.7), with photometry provided over 599 dates between 2001 February and 2009 September (more specifically, HJD 2451887 and HJD 2455088). The ASAS light curve is plotted with the SuperWASP photometry during the eclipse in Figure 4, and the entire ASAS light curve for 2001–2009 is shown in Figure 7. ASAS data also show a minor but sustained dip in magnitudes between 2001.20 and 2001.24 (~ 14 days) of approximate depth ~ 0.2 mag (see Figure 7). This magnitude difference is only 2σ above the night-to-night dispersion; however, because the dimming lasted a couple of weeks, the event stood out as unusual. If it was a true secondary eclipse, then the period should be 12.24 years and the next secondary eclipse would take place around 2013.46. High-cadence photometry of J1407

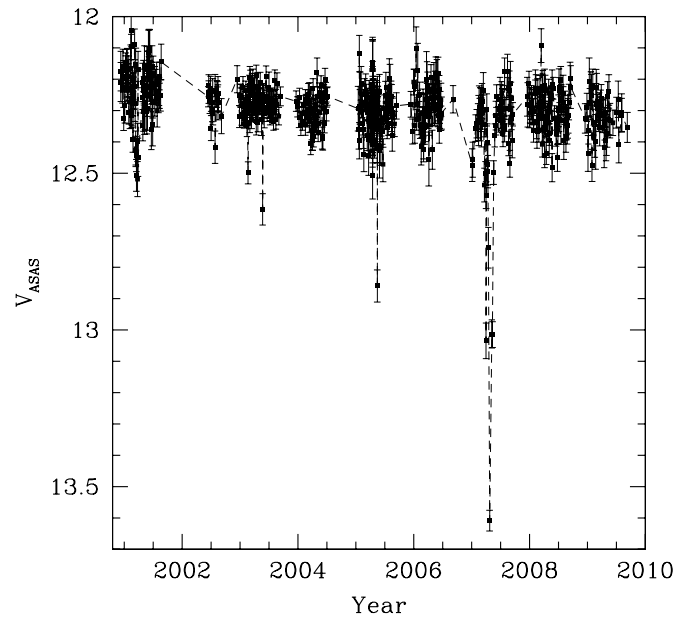


Figure 7. ASAS light curve for J1407 between 2001 February and 2009 September. An unconfirmed shallower eclipse might have occurred in early 2001. Magnitudes are reported for a given night and connected by a thin dashed line.

in mid-2013 should be able to test the idea that the 2001 event might have been a secondary eclipse.

A series of nightly V -band images were taken of J1407 with the CTIO 1.3 m telescope in queue mode during the first half of 2011. Three consecutive 10 s images were taken nightly during 106 nights between 2011 February 7 and 2011 June 22. Visual examination of the data, as well as comparison of the brightness of J1407 to neighboring stars of similar brightness, shows no evidence of deep (>0.5 mag) eclipses during this period.

3.3. Eclipse Substructure

While the deepest part of the eclipse is not well sampled in Figures 4 and 5, the eclipse of J1407 is asymmetric. Mikolajewski & Graczyk (1999) proposed that the asymmetry of EE Cep’s eclipses was due to the disk impact parameter with the line of sight, and given the similarities of the central parts of their eclipses, we suspect the same for J1407. Nightly averages of SuperWASP data (see Figure 5) exhibit two pairs of multi-day dips, labeled A_1 and A_2 , separated by ~ 24 days, and B_1 and B_2 , separated by ~ 51.5 days. Between these dips, there are periods that appear to be free of extinction lasting a few days each, indicative that there may be large gaps in the disk. Galan et al. (2010) proposed that similar dips in the 2008/2009 EE Cep eclipse were due to gaps in a multi-ring disk.

There may also be substructure on timescales shorter than a day with variations up to 1 mag on timescales shorter than a day. Figures 8 and 9 show detailed structure at the beginning and end of the eclipse. If this substructure is due to the occulting body, then it contains a remarkable wealth of structure. We have examined SuperWASP light curves of neighboring stars of similar magnitude, as well as J1407 outside of eclipse, and seen no such variations, implying that the hourly variations are due to the eclipse. We explore hypotheses to explain the eclipses in Section 3.6 and develop a model in Section 3.7.

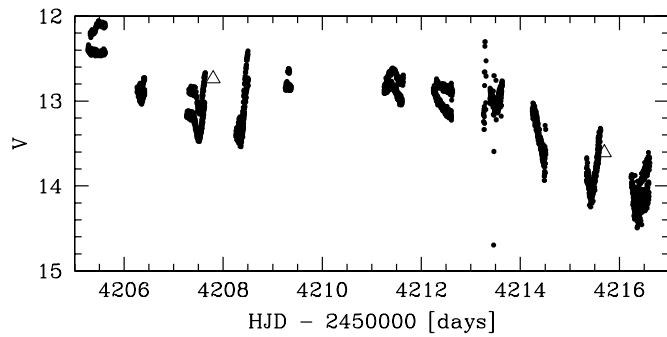


Figure 8. SuperWASP (dark filled circles) and ASAS (open triangles) photometry during the portion of the eclipse immediately before the deepest minimum. During some nights the SuperWASP photometry shows (unphysical) jumps between two photometric levels at the tenths of magnitude level—a systematic effect seen in other SuperWASP studies (e.g., Norton et al. 2011).

3.4. Rotation Period and X-Ray Emission

Young stars show variability on the timescale of days, induced by the presence of starspots on the rotating surface. Variability at the ~ 0.1 mag level can be seen in the data, so we carried out a search for periodicity in the star’s light curve to determine the star’s rotational period. The ASAS photometry and SuperWASP photometry are measured in slightly different bandpasses, and we measure this magnitude difference by taking the median magnitude of the data in each data set over the 2008 season, where there is no sign of long-term trends in the photometric light curve. We measure a systematic offset of 0.143 mag between ASAS and SWASP V -band photometry (likely due to the SWASP photometry being calibrated to the *Tycho* V_T system), so we add an offset to the SWASP photometry to put it on the ASAS V system. For the SWASP data, we calculate the median magnitude of each night and use this for the subsequent analysis.

We take the photometry from SWASP and ASAS and perform a Lomb–Scargle periodogram analysis on both data sets. False alarm probabilities (FAPs) are estimated using the method described in Press et al. (1992). The photometry over the 2008 season is shown in the top panel of Figure 10, along with the Lomb–Scargle periodograms of the SWASP and ASAS data in the lower panels. Both light curves show a highly significant periodicity of 3.20 days, with FAPs of 10^{-3} and 10^{-6} for the ASAS and SWASP data sets, respectively, with no other detectable periods seen over the sampled period ranges.

The star has an X-ray counterpart in the *ROSAT* All-Sky Survey Faint Source Catalog (RASS-FSC; Voges et al. 2000), with marginally detected flux of $f_X = 0.0359 \pm 0.0148$ counts s^{-1} and hardness ratios of $HR1 = -0.04 \pm 0.42$ and $HR2 = 0.06 \pm 0.62$. Using the energy conversion factor of Fleming et al. (1995), this translates to an X-ray flux in the *ROSAT* band of $f_X = 2.9 \times 10^{-13}$ erg s^{-1} cm^{-2} , and using our previous distance and bolometric luminosity estimates, $L_X = 10^{29.8}$ erg s^{-1} and $\log(L_X/L_{bol}) \simeq -3.4$ dex. A K5-type star with rotation period of 3.20 days would be predicted to have soft X-ray emission around the saturation level ($\log(L_X/L_{bol}) \simeq -3.2 \pm 0.3$; Pizzolato et al. 2003), perfectly consistent with the observed *ROSAT* X-ray flux ($\log(L_X/L_{bol}) \simeq -3.2$), and consistent with other Sco-Cen pre-MS stars (Mamajek et al. 2002).

3.5. Constraints on the Eclipse Period

We detect a single deep eclipse in our data set, but there is the possibility that another deep eclipse occurred during a period when there was no photometric coverage. We determine

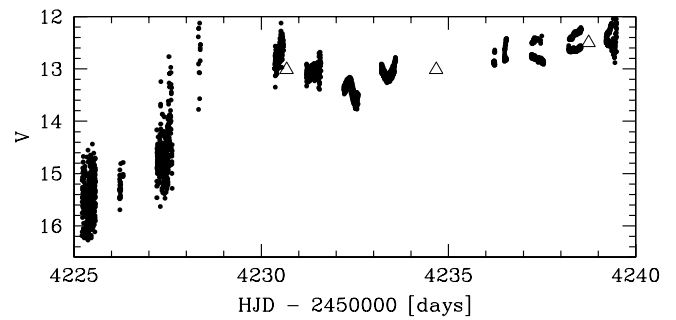


Figure 9. SuperWASP and ASAS photometry for the second part of the eclipse; the same as for Figure 8.

if there could be other eclipses that are undetected in the data set by choosing a trial period for the eclipses and plotting the light curve modulo this period. We count how many folded photometric points lie within the deepest part of the known eclipse and determine the mean magnitude and standard deviation of these points.

We define a deep eclipse event as one where the stellar magnitude fades by one magnitude or greater. For the known eclipse, we estimate that this lasts for 15 days, and we set the trial periods P for values starting at 200–2500 days in steps of 1 day. In Figure 11 we show the results of our analysis. In the upper panel we show that we have one or more photometric points for all trial periods up to 850 days, and the lower panel shows the mean magnitude of the photometric points at those periods where we have one or more photometric points. We conclude that there is no evidence for any eclipse events with photometric coverage up to 2330 days (6.4 years), and that there are no eclipse events in any periods up to 850 days (2.3 years). Approximately half of the periods between 850 days and 2330 days are ruled out (Figure 11).

If the shallow depression seen in early 2001 (see Figure 7) is an eclipse, then the period is 6.12 years and just about at the 2330 day limit. EE Cep has a similar period and duration and also exhibits variations in eclipse depth (Galan et al. 2010). Hence, we should consider the possibility that J1407 also exhibits large variations in eclipse duration and depth.

3.6. Other Explanations

The case for the primary being a pre-MS K star at $d \simeq 130$ pc seems to be secure. The primary exhibits (1) rapid rotation ($P = 3.2$ days), (2) complimentary saturated X-ray emission consistent with the rapid rotation (typical for young dwarf or pre-MS stars), (3) strong Li consistent with other pre-MS Sco-Cen members, (4) proper motion statistically consistent with Sco-Cen membership, and predicted kinematic distance harmonious with pre-MS status, and lastly (5) spectral appearance consistent with being dwarf or pre-MS, but not a giant.

Besides the apparent spectral evidence, there are reasons to exclude J1407 as a possible giant or supergiant. With these observations of the primary in mind, we briefly present and pass judgment on several hypotheses regarding the agent responsible for J1407’s unusual eclipses. If J1407 were a K5 giant with absolute magnitude similar to the K5III standards N Vel and γ Dra ($M_V \simeq -1.2$),¹¹ then its apparent V magnitude

¹¹ Using *Hipparcos* V magnitudes (Perryman & ESA 1997) and revised *Hipparcos* parallaxes (van Leeuwen 2007), we estimate that the high-quality K5III spectral standards N Vel and γ Dra (Keenan & McNeil 1989) have absolute magnitudes of $M_V \simeq -1.19$ and -1.14 , respectively, and the K5Ib standard σ Cma has $M_V \simeq -4.3$ (assuming extinction $A_V \simeq 0.12$ mag; Bobylev et al. 2006).

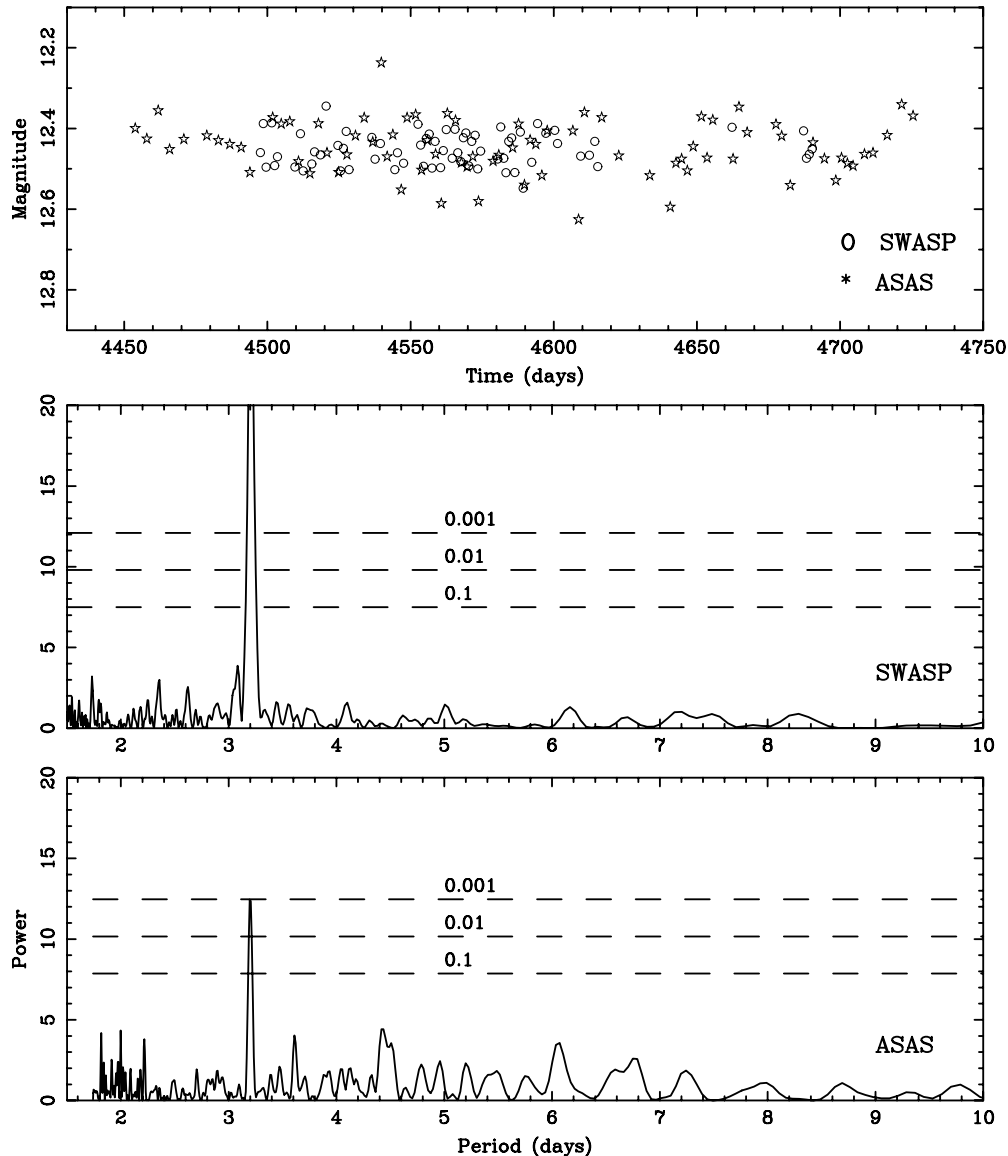


Figure 10. Top: photometry of the star over the 2008 season, where the SuperWASP (SWASP) points are daily median values. Middle: Lomb–Scargle periodogram for SuperWASP photometry. Bottom: Lomb–Scargle periodogram for the ASAS photometry. FAPs are indicated with horizontal dashed lines. A period of 3.20 days, presumably due to starspots and stellar rotation, is detected strongly and independently in both data sets.

would be consistent with a distance of ≈ 4.3 kpc. J1407’s total proper motion (32 mas yr^{-1}) would then imply a tangential velocity of $\approx 670 \text{ km s}^{-1}$, i.e., faster than the local Galactic escape velocity. Photometrically, there is no hint of long-term periodicity characteristic of red giants (i.e., Mira variability). The situation is worse if the star were a K5 supergiant. If it shared the absolute magnitude of the K5Ib standard σ CMA ($M_V \simeq -4.3$), then J1407 would represent a young, massive star ≈ 18 kpc away, ≈ 6 kpc above the Galactic disk midplane, with a tangential velocity of $\approx 2800 \text{ km s}^{-1}$. The presence of strong Li absorption, X-ray emission, and a 3 day periodicity would also seem extraordinarily unusual for a K5 giant or subgiant. Hence, we rule out J1407 being an evolved, giant, or supergiant late-K star.

We discuss some of the possible explanations for the observed eclipse and pass judgment on their plausibility.

1. *Eclipses by stellar or substellar companion alone.* No plausible stellar or substellar companion can be responsible for dimming the K5 pre-MS star J1407 by more than 3 mag

(>95% dimming), and eclipses by such an object would not explain the irregular shape, depth, and duration of the eclipse.

2. *Is the “primary” a red giant that is eclipsing a fainter, bluer star?* The rare cases of eclipsing binaries that eclipse by more than a few magnitudes are usually cases of a red giant transiting a smaller, hotter dwarf star (e.g., RV Aps; A2V+K4III; depth $\simeq 1.5$ mag; Khaliullin et al. 2006) or symbiotic binaries (e.g., AR Pav; depth $\simeq 6$ mag, period $\simeq 604$ days; Quiroga et al. 2002). There is no hint from the spectrum of J1407 that it could contain a giant star, a hot component, or constitute a symbiotic binary. As stated before, we think we can safely exclude the hypothesis that the J1407 primary is an evolved late-K giant or supergiant. Such a scenario would also not explain the eclipse structure in the weeks before and after the main deep eclipse.

3. *Could the obscuration be associated with a disk orbiting a compact stellar remnant?* The system is too young to contain a neutron star or white dwarf. Given the age of the system (~ 16 Myr), any black hole would have

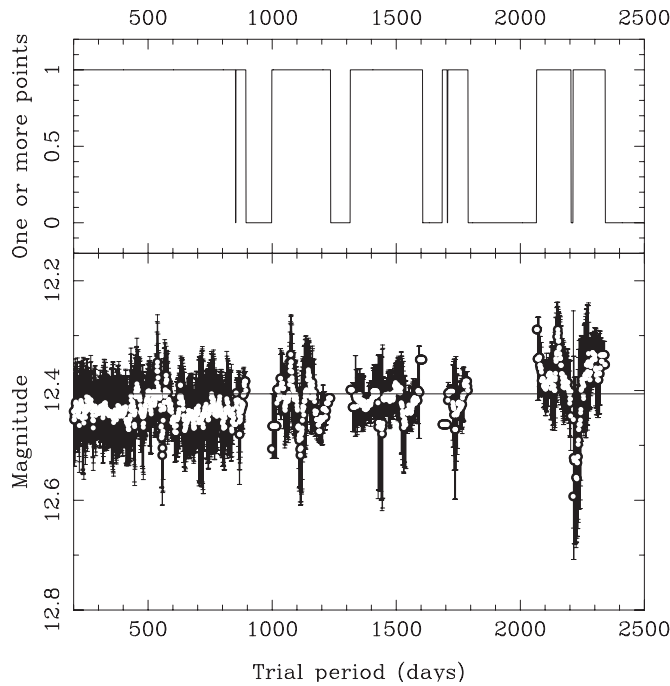


Figure 11. Photometric coverage for periodic events at different trial periods. The upper panel shows the periods where we have one or more photometric points within an eclipse event, and the lower panel shows the mean magnitude in those particular cases.

had a progenitor mass of $>14 M_{\odot}$ (Bertelli et al. 2009) and would have been an extremely large red supergiant and/or Wolf–Rayet star before its supernovae. A black hole would likely be a much stronger source of X-rays ($L_X > 10^{32} \text{ erg s}^{-1}$; Verbunt 1993) than observed ($L_X \simeq 10^{30} \text{ erg s}^{-1}$) if it accreted from a disk. Also, the system’s proper motion appears to be comoving with Sco-Cen within $\sim 1 \text{ km s}^{-1}$, so if there were a companion that supernovae and removed a substantial amount of mass from the system, then why is J1407 not a runaway star? Hence, it seems very implausible that the obscuration is associated with a disk orbiting any type of stellar remnant.

4. *Can a circumbinary or circumstellar disk about the star explain the obscuration?* The pre-MS binary system KH 15D has exhibited photometric variations and eclipses over the past half century that are attributed to the effect of a precessing circumbinary disk (Herbst et al. 2010). The eclipses are 3.5 mag deep in all bands and last for a significant fraction (one-third or 16 days) of the orbital period (48 days). The single star V718 Persei in the young cluster IC 348 also exhibits prolonged (~ 1 year) eclipses of about 1 mag with a period of 4.7 years. Its eclipses are attributed to an inner edge of a circumstellar disk (Grinin et al. 2008, 2009). For both of these systems the eclipses last a significant fraction of the orbital period, implying that the eclipsing object nearly fills the orbital plane. V718 Per has a weak IR excess corresponding to a “thin, low-mass disk” (Grinin et al. 2008). KH 15D has negligible mid-IR excess (C. Hamilton-Drager 2011, private communication). J1407 lacks a near- or mid-infrared excess that would indicate a warm dust disk of substantial optical depth (and the lack of strong emission lines in the spectrum also indicates no evidence for an accretion disk). Including the gradual dimming phase, the eclipse on J1407 lasted about 54 days. As discussed in the previous section, the period analysis

suggests that the orbital period $P > 850$ days (2.33 yr), so the ratio of eclipse duration to orbital period must be less than 0.06. This is significantly lower than the ratios for either V718 Persei or KH 15D (0.2 and 0.3, respectively) and suggests that a circumbinary or circumstellar disk about the K star cannot account for the eclipse.

5. *Could the eclipse be due to a circumstellar disk that occulted the star once owing to the relative motions of the Sun and J1407?* We have not yet positively identified more than a single eclipse, so at present it is possible that the eclipse was a one-time occurrence. As a UCL member, the tangential motion of J1407 on the sky is 32 mas yr^{-1} or 20 km s^{-1} at its predicted distance of 128 pc. What if we interpret the obscuration as being due to a geometrically thin circumstellar disk orbiting J1407, with the optical depth changing as a result of the motion of the Sun relative to J1407? The eclipse depth would then suggest an optically thick mid-plane ($\Delta \text{mag} > 3.5 \text{ mag}$, or $\tau > 3.2$). In a week, the Sun-J1407 line only sweeps 0.6 mas owing to their relative motion. Assuming the disk to be of similar size to typical planetary orbits ($\sim 10 \text{ AU}$), this would translate to sweeping the disk in the z -direction approximately $\sim 4(r_{\text{disk}}/10 \text{ AU}) \text{ km}$ per week. A two-week eclipse would correspond to a disk $\sim 10 \text{ km}$ thick, suggestive of a remarkably thin disk with an aspect ratio (height over radius) of $\sim 10^{-8}$, similar to the rings of Saturn. Besides the thinness of the disk, there are other problems with this scenario: (1) it does not explain the nearly symmetric dimmings at ± 12 and ± 26 days from the inferred eclipse minimum, (2) the similarity with the periodic eclipsing object EE Cep would have to be coincidental, and (3) the future detection of another similar eclipse would obviously negate the idea.
6. *Could the eclipses be due to a circumstellar disk orbiting a star more massive than the K5 star?* We can consider the possibility that the system is like ϵ Aurigae with the more massive object obscured by the eclipsing disk. Hiding a dwarf star more massive than the K star seen would require an edge-on disk (such as seen in images of HK Tau; Stapelfeldt et al. 1998), but again there is no evidence for an infrared excess from J1407. The $12 \mu\text{m}$ WISE flux corresponds to a flux $\lambda F_{\lambda} \sim 1.5 \times 10^{-15} \text{ W m}^{-2}$. We have used the $12 \mu\text{m}$ flux because the signal-to-noise ratio is significantly higher than that at $22 \mu\text{m}$. The error at $12 \mu\text{m}$ is only 3% of the flux, so at best a disk could be emitting with a $12 \mu\text{m}$ infrared flux of $\lambda F_{\lambda} \sim 5 \times 10^{-17} \text{ W m}^{-2}$. If only one-tenth of the disk luminosity is emitted at $12 \mu\text{m}$, then the total infrared flux of our source is at most $F_{\text{IR}} \lesssim 5 \times 10^{-16} \text{ W m}^{-2}$. The solar luminosity at a distance of 128 pc (that estimated for J1407) corresponds to $2 \times 10^{-12} \text{ W m}^{-2}$. Thus, the total infrared luminosity is at most $L_{\text{IR}} \lesssim 2.5 \times 10^{-4} L_{\odot}$. It would be difficult to hide a main-sequence star and remain below this luminosity, typical of debris disks, even if the disk were an edge-on transition disk with an inner hole. It is more likely that the object hosting the occulting disk has a lower mass than the K star. In this case, the disk infrared luminosity could be consistent with this upper limit.

3.7. A Preliminary Model

We now consider the possibility that the eclipse could be due to occultation by a circumsecondary or circumplanetary dust

disk with the secondary object and its disk in orbit about the K5 primary star (analogous to what has been proposed for EE Cep). The period analysis above suggests that the orbital period $P > 850$ days (2.33 yr), which for $m_1 = 0.9 M_\odot$ suggests an orbital radius of > 1.7 AU and an orbital velocity of < 21.7 km s $^{-1}$. The hypothetical disk appears to produce some obscuration during a minimum of $\Delta t \approx 54$ days, and hence the obscuration occurs during a fraction $f_{\text{eclipse}} < 6.3\%$ of the period. Using Equation (5) for the fraction of time spent in eclipse, we find that this limit implies that

$$m_2 \lesssim 21 M_J \xi^{-3}, \quad (8)$$

where we have used $m_1 = 0.9 M_\odot$ estimated for J1407. If the disk fills the Hill or tidal radius ($\xi \sim 1$), then the secondary is likely to be a brown dwarf. The secondary could have a higher mass if the disk radius only partly fills the tidal radius estimated from its semi-major axis. If the secondary is in an eccentric orbit and its disk is truncated tidally at pericenter, then ξ estimated from the semi-major axis would be lower than 1.

If the dimming seen in 2001 corresponds to a secondary eclipse, then the fraction of the period spent in eclipse is $f_{\text{eclipse}} \sim 0.024$, corresponding to (using Equation (5) and using an eclipse time of 54 days and period of 12 years)

$$m_2 \sim 1.2 M_J \xi^{-3}. \quad (9)$$

For $\xi \sim 0.2$ expected for circumplanetary disks this gives $m_2 \sim 0.1 M_\odot$ and an M dwarf. Both this mass estimate and the previous one estimated from the 850 day period limit suggest that the mass of the companion must be low and in the brown dwarf or low-mass M star regime. The longer the period, the lower f_{eclipse} , and the lower the estimated mass of the secondary. However, if the period is longer, then the separation between primary and secondary would be larger, making it easier to resolve using a high angular resolution imaging system. For example, a separation of 10 AU at a distance of 130 pc corresponds to 77 mas, resolvable perhaps with aperture-masking interferometry on large telescopes (e.g., Ireland & Kraus 2008).

The period and length of the eclipse can be used to estimate the disk radius. Inverting Equation (5),

$$\begin{aligned} r_d &\sim \left(\frac{t_{\text{eclipse}}}{P}\right) \left(\frac{P}{2\pi}\right)^{2/3} [G(m_1 + m_2)]^{1/3} \\ &\sim 0.08 \text{ AU} \left(\frac{f_{\text{eclipse}}}{0.06}\right) \left(\frac{P}{2.3 \text{ yr}}\right)^{2/3} \left(\frac{m_1 + m_2}{0.9 M_\odot}\right)^{1/3}. \end{aligned} \quad (10)$$

As expected, only large objects are capable of causing such a long eclipse. The disk radius is only weakly dependent on the period (proportional to $P^{-1/3}$) and would be smaller for a more distant companion.

Regions during the eclipse with little dimming could be interpreted in terms of gaps in the disk (as by Galan et al. 2010 for EE Cep). The gaps (regions labeled Z_1 , Z_2 , Y_1 , and Y_2 in Figure 5) each last a few days. The ratio of the width of these gaps to one-half of the eclipse time is approximately 3/26 or 0.11, suggesting that the disk must have an aspect ratio h/r smaller than this ratio. If we assume that the gaps are twice the Hill radius of an object embedded in the disk, then the ratio of the gap to total eclipse time gives an upper limit on the ratio of

the third power of the ratio of the satellites to secondary mass:

$$\frac{t_{\text{gap}}}{t_{\text{eclipse}}} \lesssim \left(\frac{m_s}{3m_2}\right)^{1/3}, \quad (11)$$

where m_s is the mass of the gap opening satellite. For $t_{\text{gap}}/t_{\text{eclipse}} \sim 0.06$ this corresponds to $m_s/m_2 \lesssim 10^{-3}$. If the secondary has a mass of $1 M_J$, then the satellites in the disk could have mass lower than that of Earth, and if the secondary is an M star of mass $0.1 M_\odot$, then the gap opening satellites could have mass lower than Saturn.

Photometric variations on daily timescales (e.g., see Figures 8 and 9) suggest that there are hourly variations in the eclipse depth. The ratio of a few hours (or a quarter day) to the half eclipse length is about 0.01, suggesting that the disk has an extremely low aspect ratio of $h/r \lesssim 0.01$. *If so, then the disk could not be a gaseous disk but must be a planetesimal disk or a ring system.*

We are currently attempting to model the eclipse light curve in terms of an optically thick inner disk that caused the primary deep eclipse and a system of rings of lower optical depth that caused the smaller dips in the weeks before and after the primary eclipse (E. L. Scott et al. 2012, in preparation). We have had success modeling the primary eclipse; however, the peripheral dips have been more difficult to model. Light from the primary star is modeled as a collection of spherically symmetric points (Wilson & Devinney 1971) and a secondary star or planet modeled as a sphere (we assume the tidal deformations of both objects to be negligible because the length of the eclipse and minimum period implies a large disk and distance to the primary). Limb darkening was calculated following van Hamme (1993). The disk and rings are assumed to be thin debris disks of dust with uniform density and opacity. The input parameters were the mass of the primary, the orientation of the debris disk, the orientation, period, and eccentricity of the orbit, the inner and outer radius of each ring, and the opacity of each ring. Physical parameters as a function of age and mass for the primary were taken from Baraffe et al. (1998) and for the low-mass companion from Baraffe et al. (2002).

A preliminary good fit (but by no means unique) to the daily averaged light curve for J1407 is shown in Figure 12, and the model parameters are listed in the caption and summarized in Table 5. A diagram showing the geometry of this preliminary good fit is shown in Figure 13. Besides a thick inner disk needed to explain the deep eclipse labeled C in Figure 5, our toy model includes two “rings” of different optical depths for explaining features B_1 and B_2 in the light curve. An additional optically thin outer ring is needed to explain features A_1 and A_2 in the light curve. This outer ring is not included in this model but has the following approximate parameters: $r_{\text{in}} \simeq 200R_c$ (where R_c is the companion radius, for this model assumed to be $1.46R_{\text{Jup}} \simeq 104,000$ km), $r_{\text{out}} \simeq 250R_c$, $\tau_\perp \simeq 0.09$. Another gap is needed to explain maxima Z_1 and Z_2 in Figure 5, with inner and outer radii of approximately $\sim 163R_c$ and $\sim 200R_c$.

Approximately how much dust could be responsible for the eclipses that we are seeing? The densest of Saturn’s named rings—the B ring—has a radially averaged optical depth of order unity and surface density of ~ 50 g cm $^{-2}$ (Zebker et al. 1985; de Pater & Lissauer 2001; Tiscareno 2012), implying an approximate opacity of $\kappa \sim 0.02$ cm 2 g $^{-1}$. Adopting this mass opacity for J1407’s dust annuli, the thick inner disk would have a mass of $\sim 0.8 M_{\text{Moon}}$, the two rings shown would have masses of ~ 0.2 and $\sim 0.1 M_{\text{Moon}}$, and the outermost ring would contain $\sim 0.5 M_{\text{Moon}}$ of dust mass. Our toy model assumes that the

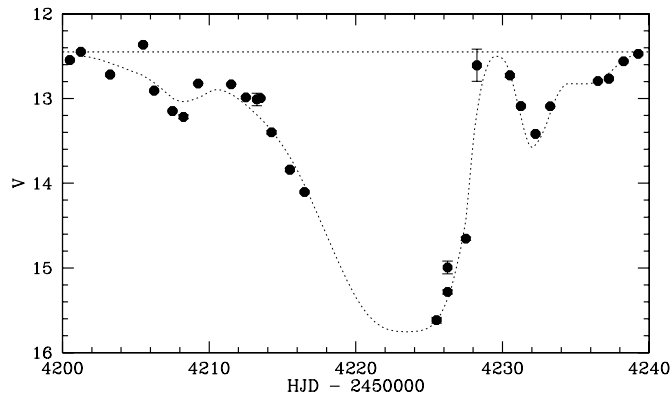


Figure 12. Simple, non-unique model attempting to fit the gross features of the nightly mean SuperWASP photometry for J1407. This model contains an object orbiting J1407 girded by a thick inner disk, a gap, and two rings with a small gap between them. The thick inner disk is used to model the deep eclipse feature “C” in Figure 5, and the two rings are modeled to fit the features “B₁” and “B₂” in the same figure. The companion object has a test orbital inclination of 89°955, axial tilt with respect to the orbital plane of 13°, orbital period 9862 days ($a = 8.7$ AU), and radius $R_c = 1.46R_{\text{Jup}}$. The model contains a thick inner disk with $\tau_{\perp} = 0.5$ and outer radius $76R_c$, a first “ring” with optical depth $\tau_{\perp} = 0.2$ between $106R_c$ and $127R_c$, and a second “ring” with optical depth $\tau_{\perp} = 0.05$ between $128R_c$ and $163R_c$. Yet another outer ring is needed to fit dips before and after the time range plotted.

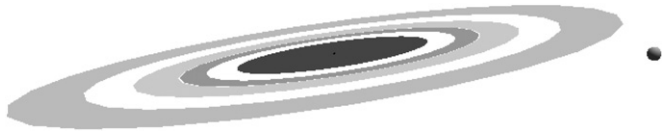


Figure 13. Diagram of J1407’s dust disk model, whose corresponding light curve is plotted in Figure 12. The K5 star J1407 is plotted to scale on the right (radius = $0.96 R_{\odot}$). The thick ($\tau = 3$) inner disk is needed to produce feature “C” in Figure 5, and the tilt is largely responsible for the asymmetric eclipse. The two annuli of lower optical depth ($\tau_{\text{perp}} = 0.2$ and 0.05) are used to fit features B₁ and B₂ in the light curve. The gap between the thick inner disk and inner ring is needed to model features Y₁ and Y₂ in Figure 5. The outer ring hypothesized to explain features A₁ and A₂ in the light curve in Figure 5 is not included in this diagram. The intra-night SuperWASP light curves are suggestive of much more substructure within the “rings” than represented here.

companion and its disk system are situated 8.7 AU from J1407; however, this is only definitively constrained to be >1.7 AU given the time-series photometry available. So any estimates of the physical scale and mass of the disk system will obviously scale with the companion’s orbital separation from J1407. For $\kappa = 0.02 \text{ cm}^2 \text{ g}^{-1}$, the total ring mass ranges from $\sim 3.6 M_{\text{Moon}}$ for $P = 2.33$ yr to $\sim 0.8 M_{\text{Moon}}$ for $P = 200$ yr. Over this same range, the outer edge of the outermost ring scales from 60 million km (0.4 AU) for $P = 2.33$ yr down to 14 million km (0.09 AU) for $P = 200$ yr. We are in the process of improving the code, attempting to fit the intra-night light curves, and making predictions of brightness of the companion’s disk in the infrared, in order to give further constraints on the size and orientation of the debris system and the physical parameters of the gaps and dust rings.

4. THE PROBABILITY OF SEEING ECLIPSES BY CIRCUMSECONDARY OR CIRCUMPLANETARY DISKS IN A SAMPLE OF YOUNG STARS

We first estimate the probability of a circumplanetary disk eclipse using probability distributions for giant planets estimated from radial velocity surveys. We then estimate the probability of a circumsecondary disk eclipse based on surveys of young binary stars.

Table 5
Ring Model Parameters

(1) Ring	(2) R_{in} (R_c)	(3) R_{out} (R_c)	(4) τ	(5) τ_{\perp}	(6) Mass (M_{Moon})
“Rochester”	1?	81	3.0	0.5	0.8
“Sutherland”	106	127	1.0	0.2	0.2
“Las Campanas”	128	163	0.3	0.05	0.1
“Tololo”	200	255	0.5	0.09	0.5

Notes. R_{in} is the inner radius, R_{out} is the outer radius, τ is the optical depth through the ring along the line of sight between the observer and the primary star, and τ_{\perp} is the optical depth through the ring perpendicular to the ring plane. Ring sizes are parameterized by companion radius, assumed to be $1.46R_{\text{Jup}}$ (104,000 km). This model assumes a companion orbital period of 27 years ($a = 9.7$ AU) and ring opacity of $\kappa = 0.02 \text{ cm}^2 \text{ g}^{-1}$. To scale the radii for different assumed orbital periods, multiply them by factor $(P/27 \text{ yr})^{-1/3}$ (where $P > 2.33$ yr). To scale the ring masses, multiply by $(P/27 \text{ yr})^{-2/3} (\kappa/0.02 \text{ cm}^2 \text{ g}^{-1})^{-1}$. Ring nicknames come from locations where observations were taken or analysis carried out for this study (the SuperWASP observations were taken using the SuperWASP-South observatory located at Sutherland, South Africa. The ASAS survey was carried out at Las Campanas Observatory, Chile. Spectra of the host star were taken with the SMARTS 1.5 m on Cerro Tololo. Discovery and analysis of the system took place at the University of Rochester).

4.1. Probability of Seeing Eclipses by Circumplanetary Disks

To estimate the probability of detecting a circumplanetary disk eclipse, we must consider the number of stars that host gas giant planets. The period and mass distribution of gas giants estimated from Doppler radial velocity surveys is

$$dN = CM^{-3.1 \pm 0.2} P^{0.26 \pm 0.1} d \log M d \log P, \quad (12)$$

where the normalization constant C is such that the fraction of FGK stars with a planet in the mass range $0.3\text{--}10 M_{\text{J}}$ (where M_{J} is a Jupiter mass) and period range $2\text{--}2000$ days is 10.5% (Cumming et al. 2008). In units corresponding to measuring planet masses in Jupiter masses and orbital periods in days, the value of the normalization is $C = 1.4 \times 10^{-3}$. Integrating over the masses, we find $dN = C' P^{0.26} d \log P$ with $C' = 4.5 \times 10^{-3}$. The distribution gives a probability of an FGK star hosting a gas giant between 1–5 AU (365–1825 days), interior to this (2–365 days), and from 5–20 AU, in each case of about $f_g \sim 0.05$ or 5%.

We consider a sample of stars restricted so that they have already depleted circumstellar disks (i.e., are post-accretion pre-MS stars) but are young enough that they could host circumplanetary disks of sufficient optical depth to produce detectable eclipses. One could choose a sample based on eliminating stars with evidence of accretion and selecting for age based on chromospheric activity, cluster, or association membership (e.g., Mamajek et al. 2002; Mamajek & Hillenbrand 2008). Typical subgroups of OB associations have $\sim 10^3$ stars and ages of $\sim 3\text{--}20$ Myr (e.g., de Zeeuw et al. 1999; Briceño et al. 2007), during which the majority of stars have just recently ceased accreting from circumstellar disks (e.g., Mamajek 2009). Light curves of post-accretion $\sim 1 M_{\odot}$ pre-MS stars in the nearest OB associations (e.g., Sco-Cen, Ori OB1, etc.) can be searched in existing SuperWASP and ASAS data sets, and indeed such an effort is currently underway by our group.

If each star in the sample is observed a single time, the fraction that would be observed in eclipse we estimate as

$f_1 \sim f_{\text{orient}} f_{\text{eclipse}} f_g$, where we multiply the number of systems with gas giants, f_g , by the fraction of orbit spent in eclipse, f_{eclipse} (Equation (5)), and fraction of orientations capable of giving eclipse, f_{orient} (Equation (3)). For our three ranges of semi-major axis radii

$$\begin{aligned} f_1 &\sim \xi^2 \mu^{2/3} 3^{-2/3} \pi^{-1} \bar{y} f_g \\ &\sim 10^{-5.8} \left(\frac{\xi}{0.2}\right)^2 \left(\frac{m_p}{M_J}\right)^{2/3} \left(\frac{M_*}{M_\odot}\right)^{2/3} \left(\frac{\bar{y}}{0.5}\right) \left(\frac{f_g}{0.05}\right). \end{aligned} \quad (13)$$

This probability is very low and implies that high-cadence monitoring of many stars is required to detect circumplanetary disk eclipses.

We now consider the same sample of stars but continuously monitor them throughout the planet’s orbital period. The fraction (for each range of semi-major axis) that would exhibit an eclipse of a circumplanetary disk would be $f_c \sim f_{\text{orient}} f_g$:

$$f_c \sim 10^{-3.7} \left(\frac{\xi}{0.2}\right) \left(\frac{m_p}{M_J}\right)^{1/3} \left(\frac{M_*}{M_\odot}\right)^{1/3} \left(\frac{\bar{y}}{0.3}\right) \left(\frac{f_g}{0.05}\right). \quad (14)$$

Restricting our study to planets between 1 and 5 AU (with $f_g \sim 0.05$) and monitoring them for 10 years (approximately the orbital time at 5 AU for $\sim 1 M_\odot$), the above fraction f_c suggests that if we monitor 10^4 stars 10^7 years old, then ~ 2 of them should exhibit circumplanetary disk eclipses.

A system with a recurring circumplanetary eclipse would make it possible to study eclipses in depth, so discovery of systems with short orbital periods is important. For example, circumplanetary disk substructure could be inverse modeled by observed high-cadence light curves during eclipse. Unfortunately, owing to the smaller Hill radius size closer to the star, we expect that the lifetime would be short for a circumplanetary disk in a smaller orbit about the star. One could search for circumplanetary disk eclipses in systems that have not yet lost their outer circumstellar disks (for example, systems such as β Pic or DM Tau). However, a circumstellar disk is a large object, and the probability that a circumplanetary disk occults the star but the circumstellar disk does not occult the star is probably even more negligible.

4.2. Probability of Seeing Eclipses by Circumsecondary Disks

We consider a 10 year photometric survey of a sample of weak-lined T Tauri stars. The fraction that would exhibit an eclipse by a disk would be the fraction that are binaries (~ 0.5 ; Duchêne et al. 2007; Kraus et al. 2011), times the fraction that have binary periods less than 10 years, times the fraction that have a secondary with an optically thick disk that could produce a significant eclipse, times the probability that such systems are oriented in a way giving eclipses (given by Equation (3)).

For young binary systems in star-forming regions the estimated fraction of mixed systems with the primary a weak-lined T Tauri star and the secondary a classical T Tauri star is not low and could be as large as $\sim 1/3$ (Monin et al. 2007). The fraction of young binary systems that have a weak-lined T Tauri primary and a secondary with a passive non-accreting disk is lower; the survey described by Monin et al. (2007) contains only 1 out of about 80 binaries. A tidally truncated disk around a low-mass secondary is expected to have a shorter accretion lifetime than the primary’s disk (Armitage et al. 1999), though

its planet formation timescale could be longer. Thus, a high mass ratio binary (with mass ratio of order $q \sim 0.1$) with a classical T Tauri phase primary and a passive disk about the secondary should be relatively rare. A mid-IR survey of about 65 binary young stars finds that about 10% contain passive dust disks (McCabe et al. 2006) and for one of these the disk is hosted by the secondary. Thus, of the binaries studied by Monin et al. (2007) and McCabe et al. (2006) we can crudely estimate that 1/100 could be like J1407 with a weak-lined T Tauri primary and a low-mass secondary with a passive disk (however, this fraction should diminish as one gets to older pre-MS stars with ages of $> 10^7$ yr). As described by Prato & Weinberger (2010), binary systems with primaries “...classified as weak-lined T Tauris, unresolved, might also harbor truncated disks around the secondary stars. Such small structures could go undetected as the result of dilution from a relatively bright primary. Circumstellar disks with central holes that show excesses in the mid-infrared but not in the near-infrared, and which do not show signatures of accretion, may be present but are effectively undetectable.” J1407 may be in this class and an example of a relatively rare young binary with weak-lined T Tauri primary and low-mass secondary hosting a passive disk.

The number of binaries is flat in log period or semi-major axis space (Halbwachs et al. 2003; Kraus et al. 2011), and young binaries are similar to field population in this respect (Duchêne et al. 2007). Based on this distribution, about 1/3 of all binaries have periods less than 10 years (dividing the semi-major axis ranges into three ranges 1–10 yr, 10–100 yr, and 100–1000 yr). Thus, the number of weak-lined T Tauri stars that are binaries with periods less than 10 years and contain low-mass secondaries with passive disks would be of order 1/600. Using a mass ratio of 0.1, $\bar{y} = 0.3$, and $\xi = 1$, we estimate the fraction oriented such that they can give eclipses $f_{\text{orient}} \sim 0.1$. Altogether a 10 year survey of weak-lined T Tauri stars might have a probability of detecting an eclipse of order 1/6000, giving a similar probability to that estimated above for circumplanetary disk eclipses. An estimate folding the mass distribution and lifetime distributions would improve this estimate. However, this is difficult to formulate as binary identifications are not complete at mass ratios less than 0.1 (e.g., Kraus et al. 2011) and the number of secondaries hosting passive disks in the 10^7 year old age range is not well characterized. There are hints that the protoplanetary disk fraction decay timescale is systematically longer for lower-mass stars and brown dwarfs compared with Sun-like stars and massive stars (Mamajek 2009); however, further observations will be useful in constraining these findings for components of binary systems.

5. CONCLUSION

In this study, we have estimated the probability that a system hosting a gaseous circumplanetary or circumsecondary disk about a planet could occult a star. The existence of circumplanetary disks after the dissipation of the protosolar (circumstellar) nebular disk has been postulated from formation scenarios for the Galilean satellites (Canup & Ward 2002; Magni & Coradini 2004; Ward & Canup 2010). Because such a disk would be large, the probability that a system hosting one is oriented in such a way that it can occult the star is tiny, but not zero. Because the lifetime of a circumplanetary disk could be longer for planets at large semi-major axis, light detected from outer exoplanets such as Fomalhaut b may arise from such a disk. We estimate that eclipses from the thick inner circumplanetary disks that spawn regular satellite systems

around gas giants may last for days; however, tenuous outer disks of lower optical depths to larger fractions of the Hill radius could persist for weeks, depending on the planet's mass and semi-major axis. We estimate that a survey monitoring 10^4 stars that are approximately 10^7 years old for 10 years would likely yield at least a few circumplanetary and circumsecondary disk eclipse candidates. The 8.4 m Large Synoptic Survey Telescope (LSST; Ivezić et al. 2008) will photometrically monitor many thousands of pre-MS stars in cataloged OB associations, young star clusters, and star-forming regions during its scans of the Galactic plane region. The LSST survey design should enable estimation of sub-mas/yr proper motions that will allow kinematic membership assignments of newly discovered pre-MS stars to young clusters and associations of determinable distance and age. Optical spectroscopic follow-up will be necessary to confirmation of youth (via Li absorption; see our study of J1407) and estimation of reddening for confirming that the star has luminosity and isochronal age consistent with the other cluster/association members. Even given LSST's proposed field revisit time (~ 3 days, but twice per night), a J1407-like eclipse would have been easily detected. Higher cadence follow-up imaging from smaller dedicated telescopes will be necessary for detailed characterization of the eclipse light curves, but LSST monitoring of young stellar groups should yield some candidate disk eclipse objects.

In a survey of a few hundred 10^7 year old stars we have discovered a deep long eclipse in 2007 on the pre-MS K dwarf star J1407. This star was selected to be in the appropriate age range and could host either a circumplanetary disk or a lower mass secondary star with a disk. The lack of infrared emission suggests that the mass of the unseen object is much lower than that of the solar-mass K star. Limits for the period and the observed eclipse time suggest that the unseen object hosting the disk is low mass, perhaps in the substellar regime. Substructure in the eclipse suggests that the disk is thin $h/r \lesssim 0.01$ and has gaps that may contain satellites with mass $\sim 10^{-3}$ times that of the secondary. Follow-up with a radial velocity study is important as radial velocity measurements could put limits on both the period and mass of the secondary.

The complex eclipse of J1407 that took place in 2007 is slightly asymmetric and contains significant substructure, similar to the eclipses of the Be star EE Cep that have been interpreted in terms of an occulting planetary system (Galan et al. 2010). As has been proposed for this system, the asymmetry of the eclipse could be due to the impact parameter of the disk with respect to the line of sight (Mikolajewski & Graczyk 1999). Variations in eclipse depth in this system are attributed to a possible third companion that tilts the orbital plane of the eclipsing system (Torres & Stefanik 2000). Identifying a second eclipse for J1407 will allow measurement of the eclipse period and planning of observing campaigns similar to those launched for EE Cep and ϵ Aurigae.

Constraints from the gas giant satellite systems in our own solar system suggest that their circumplanetary disk structures could have produced quite complex eclipses if seen in transit, with dense inner regions, gaps where satellite formation is taking place, and low-density disks possibly extending to large fractions of the Hill radius. Such eclipses seen among young stars may provide remarkable laboratories for testing satellite and planet formation scenarios. Regardless of the nature of the disked companion of J1407 (low-mass star, brown dwarf, or gas giant planet), detailed observations of future eclipses should provide useful constraints on either circumsecondary or

circumplanetary disk structure and the early evolution of planets and/or satellites.

We have used data from the WASP public archive in this research. The WASP consortium comprises the University of Cambridge, Keele University, University of Leicester, The Open University, The Queen's University Belfast, St. Andrews University, and the Isaac Newton Group. Funding for WASP comes from the consortium universities and from the UK's Science and Technology Facilities Council. The star exhibiting the unusual eclipse was discovered in a spectroscopic survey using the SMARTS 1.5 m telescope at Cerro Tololo, and the survey and support for E.M. and M.P. were funded by NSF award AST-1008908. E.M., M.P., F.M., and E.S. acknowledge support from the University of Rochester College of Arts and Sciences. A.Q. acknowledges support through NSF award AST-0907841. This research has made use of the NASA/IPAC Infrared Science Archive, which is operated by the Jet Propulsion Laboratory, California Institute of Technology, under contract with the National Aeronautics and Space Administration. E.M. also thanks David James, John Subasavage, Andrei Tokovinin, Warren Brown, and Catrina Hamilton-Drager for discussions, and Fred Walter for scheduling queue observations of the star and standards on the SMARTS 1.5 m.

Facilities: SuperWASP, ASAS, CTIO:1.5m, CTIO:1.3m

REFERENCES

- Agnor, C. B., & Hamilton, D. P. 2006, *Nature*, **441**, 192
 Alibert, Y., Mousis, O., & Benz, W. 2005, *A&A*, **439**, 1205
 Anderson, J. D., Lau, E. L., Sjogren, W. L., Schuber, G., & Moore, W. B. 1996, *Nature*, **384**, 541
 Andrews, S. M., Czekala, I., Wilner, D. J., et al. 2010, *ApJ*, **710**, 462
 Armitage, P. J., Clarke, C. J., & Tout, C. A. 1999, *MNRAS*, **304**, 425
 Arnold, L., & Schneider, J. 2004, *A&A*, **420**, 1153
 Artymowicz, P., & Lubow, S. H. 1994, *ApJ*, **421**, 651
 Augereau, J. C., & Papaloizou, J. C. B. 2004, *A&A*, **414**, 1153
 Ayliffe, B. A., & Bate, M. R. 2009, *MNRAS*, **397**, 657
 Backman, D. E., & Gillett, F. C. 1985, *ApJ*, **299**, L99
 Baraffe, I., Chabrier, G., Allard, F., & Hauschildt, P. H. 1998, *A&A*, **337**, 403
 Baraffe, I., Chabrier, G., Allard, F., & Hauschildt, P. H. 2002, *A&A*, **382**, 563
 Barnes, J. W., & Fortney, J. J. 2004, *ApJ*, **616**, 1193
 Bate, M. R., Bonnell, I. A., Clarke, C. J., et al. 2000, *MNRAS*, **317**, 773
 Bertelli, G., Nasi, E., Girardi, L., & Marigo, P. 2009, *A&A*, **508**, 355
 Bessell, M. S. 2000, *PASP*, **112**, 961
 Bobylev, V. V., Goncharov, G. A., & Bajkova, A. T. 2006, *Astron. Rep.*, **50**, 733
 Briceño, C., Preibisch, T., Sherry, W. H., et al. 2007, in *Protostars and Planets V*, ed. B. Reipurth, D. Jewitt, & K. Keil (Tucson, AZ: Univ. Arizona Press), 345
 Butters, O. W., West, R. G., Anderson, D. R., et al. 2010, *A&A*, **520**, L10
 Canup, R. M., & Ward, W. R. 2002, *AJ*, **124**, 3404
 Castillo-Rogez, J., Johnson, T. V., Lee, M. H., et al. 2009, *Icarus*, **204**, 658
 Chadima, P., Harmanec, P., Bennett, P. D., et al. 2011, *A&A*, **530**, A146
 Chen, C. H., Mamajek, E. E., Bitner, M. A., et al. 2011, *ApJ*, **738**, 112
 Chiang, E., Kite, E., Kalas, P., Graham, J. R., & Clampin, M. 2009, *ApJ*, **693**, 734
 Clampin, M., Krist, J. E., Ardila, D. R., et al. 2003, *AJ*, **126**, 385
 Cumming, A., Butler, R. P., Marcy, G. W., et al. 2008, *PASP*, **120**, 531
 Cutri, R. M., Skrutskie, M. F., van Dyk, S., et al. 2003, *VizieR Online Data Catalog*, **2246**, 0
 D'Antona, F., & Mazzitelli, I. 1997, *Mem. Soc. Astron. Ital.*, **68**, 807
 de Pater, I., & Lissauer, J. J. 2001, *Planetary Sciences* (Cambridge: Cambridge Univ. Press), 544
 de Zeeuw, P. T., Hoogerwerf, R., de Bruijne, J. H. J., Brown, A. G. A., & Blaauw, A. 1999, *AJ*, **117**, 354
 Duchêne, G., Delgado-Donate, E., Haisch, K. E., Jr., Loinard, L., & Rodriguez, L. F. 2007, in *Protostars and Planets V*, ed. B. Reipurth, D. Jewitt, & K. Keil (Tucson, AZ: Univ. Arizona Press), 379
 Edgar, R. G., Quillen, A. C., & Park, J. 2007, *MNRAS*, **381**, 1280
 Fleming, T. A., Schmitt, J. H. M. M., & Giampapa, M. S. 1995, *ApJ*, **450**, 401

- Galan, C., Mikolajewski, M., Tomov, T., et al. 2010, in Proc. Conf. held 2009 June 8–12 in Brno, Czech Republic, Binaries—Key to Comprehension of the Universe, ed. A. Prša & M. Zejda (San Francisco, CA: ASP), 423
- Graczyk, D., Mikolajewski, M., Tomov, T., Kolev, D., & Iliev, I. 2003, *A&A*, 403, 1089
- Graczyk, D., Soszyński, I., Poleski, R., et al. 2011, *Acta Astron.*, 61, 103
- Grinin, V., Stempels, H. C., Gahm, G. F., et al. 2008, *A&A*, 489, 1233
- Grinin, V. P., Arkharov, A. A., Barsunova, O. Y., & Sergeev, S. G. 2009, *Astron. Lett.*, 35, 828
- Guinan, E. F., & DeWarf, L. E. 2002, in ASP Conf. Ser. 279, Exotic Stars as Challenges to Evolution, ed. C. A. Tout & W. van Hamme (San Francisco, CA: ASP), 121
- Halbwachs, J. L., Mayor, M., Udry, S., & Arenou, F. 2003, *A&A*, 397, 159
- Hartigan, P., & Kenyon, S. J. 2003, *ApJ*, 583, 334
- Herbst, W., LeDuc, K., Hamilton, C. M., et al. 2010, *AJ*, 140, 2025
- Ireland, M. J., & Kraus, A. L. 2008, *ApJ*, 678, L59
- Ivezic, Z., Tyson, J. A., Acosta, E., et al. 2008, arXiv:0805.2366
- Kalas, P., Graham, J. R., Chiang, E., et al. 2008, *Science*, 322, 1345
- Keenan, P. C., & McNeil, R. C. 1989, *ApJS*, 71, 245
- Kennedy, G. M., & Wyatt, M. C. 2011, *MNRAS*, 412, 2137
- Khaliullin, Kh. F., Khaliullina, A. I., Pastukhova, E. N., & Samus, N. N. 2006, *IBVS*, 5722, 1
- Kloppenborg, B., Stencel, R., Monnier, J. D., et al. 2010, *Nature*, 464, 870
- Kraus, A. L., Ireland, M. J., Martinache, F., & Hillenbrand, L. A. 2011, *ApJ*, 731, 8
- Lin, D. N. C., & Papaloizou, J. C. B. 1993, in Protostars and Planets III, ed. E. Levy & M. S. Matthews (Tucson, AZ: Univ. Arizona Press), 749
- Magni, G., & Coradini, A. 2004, *Planet. Space Sci.*, 52, 343
- Mamajek, E. E. 2005, *ApJ*, 634, 1385
- Mamajek, E. E. 2009, in AIP Conf. Ser. 1158, Exoplanets and Disks: Their Formation and Diversity (Melville, NY: AIP), 3
- Mamajek, E. E., & Hillenbrand, L. A. 2008, *ApJ*, 687, 1264
- Mamajek, E. E., Meyer, M. R., & Liebert, J. 2002, *AJ*, 124, 1670
- Martin, R. G., & Lubow, S. H. 2011, *MNRAS*, 413, 1447
- Massey, P. 2002, *ApJS*, 141, 81
- McCabe, C., Ghez, A. M., Prato, L., et al. 2006, *ApJ*, 636, 932
- Mikolajewski, M., Galan, C., Gazeas, K., et al. 2005, *Ap&SS*, 296, 445
- Mikolajewski, M., & Graczyk, D. 1999, *MNRAS*, 303, 521
- Monin, J.-L., Clarke, C. J., Prato, L., & McCabe, C. 2007, in Protostars and Planets V, ed. B. Reipurth, D. Jewitt, & K. Keil (Tucson, AZ: Univ. Arizona Press), 395
- Mosqueira, I., Estrada, P., & Turrini, D. 2010, *Space Sci. Rev.*, 153, 431
- Norton, A. J., Payne, S. G., Evans, T., et al. 2011, *A&A*, 528, A90
- Ohta, Y., Taruya, A., & Suto, Y. 2009, *ApJ*, 690, 1
- Pecaut, M. J., Mamajek, E. E., & Bubar, E. J. 2011, *ApJ*, in press (arXiv:1112.1695)
- Perryman, M. A. C., & ESA. 1997, in The Hipparcos and Tycho Catalogues (ESA Special Publication, Vol. 1200; Noordwijk: ESA)
- Pizzolato, N., Maggio, A., Micela, G., Sciortino, S., & Ventura, P. 2003, *A&A*, 397, 147
- Pojmanski, G. 2002, *Acta Astron.*, 52, 397
- Pollacco, D. L., Skillen, I., Cameron, A. C., et al. 2006, *PASP*, 118, 1407
- Prato, L., & Weinberger, A. J. 2010, in Planets in Binary Star Systems, ed. N. Haghighipour (Astrophysics and Space Science Library, Vol. 366; Berlin: Springer), 1
- Preibisch, T., & Mamajek, E. 2008, Handbook of Star Forming Regions, Vol. II, ed. B. Reipurth (San Francisco, CA: ASP), 235
- Press, W. H., Teukolsky, S. A., Vetterling, W. T., & Flannery, B. P. 1992, Numerical Recipes in FORTRAN: The Art of Scientific Computing (2nd ed.; Cambridge: Cambridge Univ. Press)
- Quillen, A. C. 2006, *MNRAS*, 372, L14
- Quillen, A. C., & Trilling, D. E. 1998, *ApJ*, 508, 707
- Quillen, A. C., Varniere, P., Minchev, I., & Frank, A. 2005, *AJ*, 129, 2481
- Quiroga, C., Mikolajewska, J., Brandi, E., Ferrer, O., & Garcia, L. 2002, *A&A*, 387, 139
- Roeser, S., Schilbach, E., Schwan, H., et al. 2008, *A&A*, 488, 401
- Siess, L., Dufour, E., & Forestini, M. 2000, *A&A*, 358, 593
- Skrutskie, M. F., Cutri, R. M., Stiening, R., et al. 2006, *AJ*, 131, 1163
- Stapelfeldt, K. R., Krist, J. E., Menard, F., et al. 1998, *ApJ*, 502, L65
- The DENIS Consortium. 2005, VizieR Online Data Catalog, 2263, 0
- Tiscareno, M. S. 2012, in Planets, Stars and Stellar Systems, ed. P. Kalas & L. French, in press (arXiv:1112.3305)
- Torres, G., & Stefanik, R. P. 2000, *AJ*, 119, 1914
- van Hamme, W. 1993, *AJ*, 106, 2096
- van Leeuwen, F. 2007, in Hipparcos, the New Reduction of the Raw Data (Astrophysics and Space Science Library, Vol. 350; Berlin: Springer)
- Verbunt, F. 1993, *ARA&A*, 31, 93
- Voges, W., Aschenbach, B., Boller, T., et al. 1999, *A&A*, 349, 389
- Voges, W., Aschenbach, B., Boller, T., et al. 2000, *IAU Circ.*, 7432, 3
- Ward, W. R., & Canup, R. M. 2010, *AJ*, 140, 1168
- Wilson, R. E., & Devinney, E. J. 1971, *ApJ*, 166, 605
- Wright, E. L., Eisenhardt, P. R. M., Mainzer, A. K., et al. 2010, *AJ*, 140, 1868
- Zacharias, N., Finch, C., Girard, T., et al. 2010, *AJ*, 139, 2184
- Zebker, H. A., Marouf, E. A., & Tyler, G. L. 1985, *Icarus*, 64, 531